VOL. 4 No. 9 SEPTEMBER 1939

Philips Technical Review

DEALING WITH TECHNICAL PROBLEMS
RELATING TO THE PRODUCTS, PROCESSES AND INVESTIGATIONS OF
N.V. PHILIPS' GLOEILAMPENFABRIEKEN

EDITED BY THE RESEARCH LABORATORY OF N.V. PHILIPS' GLOEILAMPENFABRIEKEN, EINDHOVEN, HOLLAND

THE PROPAGATION OF WIRELESS WAVES ROUND THE EARTH

By BALTH. van der POL and H. BREMMER.

621.396.11

This article discusses the results of calculations made to investigate the effect of the curvature of the earth on the propagation of radio waves, with special reference to the effect of the height of the transmitter and the receiver above ground level, the wave length, the electrical constants of the soil, and the distance traversed. The atmosphere is regarded as a homogeneous dielectric, thus neglecting reflexion at the ionosphere and refraction in the troposphere. It is found that the diffraction of wireless waves is so pronounced that it is almost immaterial whether the receiver is a short distance in front of or somewhat behind the optical horizon. Only for waves below 1 cm are there definite indications of a sharp cut-off limit in the distribution of field strength.

Introduction

When, in 1901, Marconi after several fruitless attempts succeeded in picking up on the Coast of Newfoundland wireless signals which had been sent out from Ireland, a distance of 2 100 miles away, the question naturally arose as to the means by which electromagnetic waves were able to traverse such a long distance, since the curvature of the earth prevented a straight path being followed between the transmitting and receiving stations (see *fig. 1*).

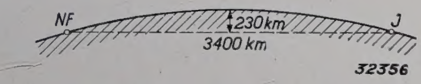

Fig. 1. The elevation of the earth between Ireland and Newfoundland appears to be equivalent to a mountain 144 miles high.

The problem soon attracted the attention of several leading mathematicians and physicists, including Poincaré, Macdonald, Nicholson Love and Sommerfeld, for the ease with which the waves were able to overcome the curvature of the earth appeared inexplicable, since in optical terms the receiving station was located well within the "shadow region". Heaviside and Kennelly had readily suggested that at a high level the atmosphere contained a conducting layer which assisted the waves to overcome the curvature of the earth. We now know that this explanation was right, but at the time it was advanced it was regarded with very grave doubt by many authorities. The easiest way of deciding the question was to compare the actual field strength of the waves at a considerable distance from the transmitter with the field strength obtained theoretically on the assumption of pure diffraction of the waves round the surface of the earth, *i.e.* without assuming a reflecting layer as proposed by Kennelly and Heaviside. For years, the investigators mentioned above devoted the closest study to this theoretical problem, which may be formulated as follows: Given a radio transmitter with a known output, to determine the field strength at any arbitrary point beyond the station on or above the earth's surface, assuming the atmosphere to be perfectly homogeneous and non-conducting, *i.e.* in the absence of the layer which is now distinguished as the ionosphere. Years of research were needed before this field strength could be calculated, because the solution of the problem obtained by classical analysis, assumed a form unsuited to numerical computation.

The general solution, in which the conductivity of the earth may have an arbitrary value, can be expressed by an infinite series of spherical harmonics, in which each term has an expression containing 12 Bessel functions as coefficient. Moreover, the nature of this series is such that each term roughly cancels out the one preceding it by reversal of the algebraical sign, so that the sum of the small differential remainders actually determines the final value sought. It is also found that the final value is not determined in the main by the initial terms of the series, but by those terms whose order in the series lies in the region of the ratio of the earth's circumference to the wave length used, *i.e.* in the region of the 100 000th or millionth term.

Although from the very outset there was general agreement as to the composition of this extremely complex series, opinions as to its numerical interpretation were so divergent that two distinct schools of thought developed. According to one school, diffraction of the waves round the earth accounts for the experimental results obtained, while the other school considered diffraction as inadequate alone and believed that the assumption of a conducting ionosphere was essential. The views of mathematicians on this problem differed so widely that in 1910 Nicholson stated that in the whole field of mathematical analysis there was no other problem, upon the solution of which such divergent opinions had been advanced.

One of the fundamental difficulties of the problem was that of finding satisfactory approximations for the Bessel functions occurring in the coefficients of the terms of the series; in 1918, Watson applying a new method succeeded in integrating the series, which brought the problem considerably nearer to a numerical solution. A critical investigation made by one of the present authors in 1919, in the course of which the whole of the available experimental and theoretical evidence was carefully sifted and compared, led to the definite conclusion that in radio-transmission experiments over long distances the presence of a conducting ionosphere was imperative and had a very helpful effect. This did not signify that all interest in the theoretical problem of pure diffraction of the waves about the surface of a sphere was vitiated, for it soon appeared that the action of the ionosphere was mainly operative during the night, and that during the day waves from 200 to 2 000 m were largely absorbed by the ionosphere and not reflected back to the earth's surface; a behaviour due to the change in the distribution of ionisation under the action of solar rays. Thus for the waves in question conditions during hours of daylight are roughly those obtaining in the absence of the ionosphere. Calculation of the field strength during the day at long distances and for the wave band in question is in fact still carried out by methods which neglect the presence, and hence the action, of the ionosphere.

Subsequently, the suitability of still shorter waves for radio communication was discovered, *viz.*, those with wave lengths between 10 and 100 m, and it appeared that their propagation was promoted, during the day also, by still higher ionised layers, which were actually found by Appleton. On passing over to ultra-short waves with wave lengths below 10 m, as used nowadays for television, a range is reached in which the ionosphere exercises no influence either during the day or the night, so that the problem was again reduced to pure diffraction phenomena, which form the subject of the present article. The technical application of waves below 10 m, which will apparently be employed on an increasing scale in the future, led us to take up this problem again, in order to make a computation of the propagation of these short waves round a television transmitter to distances up to the visible horizon and beyond.

The purpose of the present article is to give an abstract and a review of the numerical results of our calculations which have been published elsewhere [1]). In these calculations, the earth has been regarded as perfectly spherical, all topographical inequalities thus being neglected. It was also assumed that the earth is electrically homogeneous, *i.e.* composed of the same soil or covered with water over its whole surface.

The third simplification made in the simple analysis to which principal attention will be directed here, is that the atmosphere, too, is homogeneous. Two phenomena have, therefore, been neglected, *viz.*, the effect of the ionosphere and the diffraction occurring in the lower layers of the atmosphere, where diffraction is produced, as in optics, as a result of variations in density and temperature, and hence in electrical characteristics, with increasing height in this lower atmosphere or troposphere. Owing to this phenomenon, short waves in particular have a greater range than in a homogeneous atmosphere. This assumption of a homogeneous atmosphere imposes a very far-reaching restriction which, however, as already pointed out, is tolerable in many cases. In radio practice, the presence or absence of atmospheric action becomes mainly apparent by the occurrence or absence of fading phenomena.

The significance of the simplifications made here to the mathematical treatment of the problem is that the earth is replaced by a sphere whose electromagnetic behaviour can be represented by two constants, which have the same value at all points over its surface; these constants are the electrical conductivity σ and the dielectric constant ε. In other words, the earth is regarded as a medium which can act simultaneously as a conductor and as a dielectric, exactly as, for instance, in a cable with surface leakage currents in the transverse direction the medium between the sheath and the conducting core behaves as a dielectric and as a conductor at one and the same time.

---

[1]) Balth. van der Pol and H. Bremmer Phil. Mag. **24,** 141 and 825, 1937; **25,** 817, 1938; **27,** 261, 1939, *Cf.* also bibliography at the end of this paper.

The small conductivity of the troposphere, has practically no influence on wave propagation, whilst the dielectric constant differs only little from unity. Thus if the action of the ionosphere may be neglected we can substitute the ether for the troposphere and take $\varepsilon = 1$ and $\sigma = 0$.

Analogy to Similar Problems

With the assumptions made above, the problem of wave propagation may be formulated as follows: Given a source of electromagnetic waves (a transmitter) situated outside a sphere, to determine the intensity of the electromagnetic field on the sphere or at a point a short distance above it (*i.e.* at the point of reception). Various phenomena are known which may be regarded as mathematically analogous to this problem, *viz.*, all such phenomena in which the path of wave propagation suffers interference at a spherical obstruction; examples of these phenomena are the scattering of light by small spherical particles as in a colloidal solution, the dispersion of sunlight by spherical raindrops as in the formation of rainbows, and the dispersion of acoustic waves by a spherical obstruction, *e.g.* a microphone. While the strict mathematical solutions of these problems are more or less similar, differences appear in the numerical results mainly because two classes of magnitudes differ in each problem; firstly, a geometrical magnitude, *viz.*, the ratio of the circumference of the spherical obstruction to the wave length, and, secondly, two physical magnitudes: the manner in which the waves are reflected at the surface as well as the way in which the waves penetrating the sphere are absorbed. Thus, in a geometrical sense, there is a great similarity between wave propagation in radio and in the optical phenomena in the case of the rainbow [2]), the ratio of the earth's circumference to the mean wave length of wireless waves being of the same order of magnitude as the ratio of the circumference of the raindrop to the wave length of visible light. Owing to the great value of this ratio, only a very small proportion of the waves is bent round the sphere in both cases. Yet, all other physical conditions in the two cases are entirely different, since a wireless wave on penetrating the earth is very rapidly absorbed, while a ray of light can pass practically without hindrance through a raindrop. In consequence, several rays are produced from a single incident light ray in a rainbow, because a ray entering a raindrop gives rise to new rays by reflection at the surface, while in radio propagation reflected waves have such a weak intensity that they become insignificant. Apart from directly incident radiation, the only other rays of importance in practice are those produced by direct reflection; all other wireless waves (shown by broken lines in *fig. 2*) are so weak that they are not detectable.

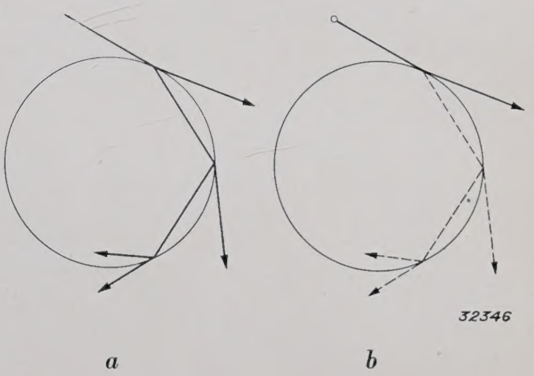

Fig. 2. *a*. Reflexion and refraction of a ray of light by a raindrop. *b*. Reflexion and refraction of a wireless wave at the earth's surface. In the second case the penetrating ray is strongly absorbed, so that only the once-reflected ray is important.

Calculations for Points of Reception Close to or Beyond the Optical Horizon of the Transmitter

In the case of wireless waves, the practical evaluation of the infinite series referred to above gives fundamentally different formulae, if the point of reception is close to or within the optical horizon of the transmitter, or if this point is beyond the horizon. The series of spherical harmonics forming the starting point of all calculations can be transformed into a new, more rapidly converging series when the point of reception is beyond the optical horizon, and if the point of reception is far enough beyond the horizon only a single term is required. If, moreover, the transmitter and receiver are both situated at ground level calculation is fairly simple. The field strength in milli-volts per metre at a receiving point distant D km from a transmitter radiating on a power level of P kilowatts, is then expressed by:

---

[2]) This analogy has also enabled us to develop from the theoretical analysis of the radio problem a corresponding new and strict theory of the rainbow. This theory shows, *inter alia*, that on observing the rainbow through polaroid spectacles that part of the bow disappears which is directed vertically to the direction of polarisation.

$$E_{\mathrm{mV/m}} = \frac{300\,\sqrt{P_{\mathrm{kW}}}}{D_{\mathrm{km}}} \cdot f(\lambda, \sigma, \varepsilon, D), \quad . \quad . \quad (1)$$

where f is a function dependent on the wave length λ, the conductivity σ and the dielectric constant ε of the soil and on the distance [3]. In the case under consideration function f has approximately the form:

$$f(\lambda, \sigma, \varepsilon, D) = \\ = 0.2905\,\frac{\sqrt{D_{\mathrm{km}}}}{\lambda_{\mathrm{m}}^{1/6}}\,\frac{e^{-0.0537\,\beta\,D_{\mathrm{km}}/\lambda_{\mathrm{m}}^{1/3}}}{\sqrt{\alpha^2 + \left(\beta - \dfrac{9.75 \cdot 10^{-9}}{\sigma_{\mathrm{EMU}}\,\lambda_{\mathrm{m}}^{5/3}}\right)^2}}\,, \quad \cdot \quad (2)$$

where α and β are magnitudes which can be derived from the graph in *fig. 3* for given values of σ and λ. Although α and β depend on σ, they are not dependent on ε, so that the dielectric constant does not appear in the approximation of function f given here. This means that the earth has been regarded as a conductor or the displacement currents, generated in the earth, have been neglected with reference to the conduction currents, as expressed by the second condition given below. The difference between the exact solution and equation (1) is less than 10 per cent if the following conditions are satisfied:

1) The distance D_{km} of the transmitter from the point of reception is greater than $40\ \lambda_{\mathrm{m}}^{1/3}$;
2) This distance D_{km} is smaller than

$$0.6 \cdot 10^{14} \cdot \frac{\sigma_{\mathrm{EMU}}\ \lambda_{\mathrm{m}}^{4/3}}{\varepsilon}\,.$$

This restriction applies particularly with long waves in propagation over water (where ε has the very high value of 80), as well as with short waves in propagation over low-conducting ground (σ_{EMU} of the order of 10^{-14}); and

3) Both transmitter and receiver are at ground level.

The factor $300\ \sqrt{P_{\mathrm{kW}}}/D_{\mathrm{km}}$ which occurs in equations (1) and (3) gives the field strength obtaining with a flat earth possessing infinite conductivity, which means that reflection losses can be neglected. The factor $f\ (\lambda,\ \sigma,\ \varepsilon,\ D)$ expresses the deviations caused by the spherical shape of the earth and due to the fact that not the whole of the radiation incident on it is reflected, but a portion refracted towards the earth's core. In view of this spherical shape, the field with the transmitter and receiver both at ground level, as assumed here, can only reach the point of reception by diffraction of the waves radiated from the transmitter. Yet, in general, the reduction in field strength with increasing distance due to absorption exceeds the reduction due to the increasing diffraction of the waves necessary in order to reach the point of reception. For short waves, one may state that the curvature of the earth has practically no influence upon wave propagation within the whole range of the transmitter, which practically is determined by absorption alone.

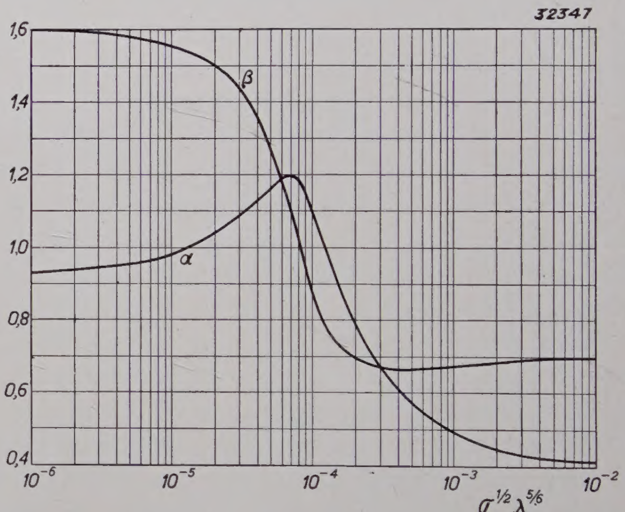

Fig. 3. Coefficients β of equation (1) plotted as a function of $\sigma_{\mathrm{EMU}}^{1/2}\ \lambda_{\mathrm{m}}^{5/6}$, where σ is the conductivity of the soil and λ_{m} is the wave length in m.

The alteration in the field strength when either the transmitter or receiver is raised above the surface, their distance apart remaining the same, can also be investigated. At distances far beyond the horizon of the transmitter, the field strength then to a first approximation increases by a factor which is independent of the distance D and is determined solely by the height of the transmitter and receiver above the surface. This height-gain factor is the product of a factor expressing the effect of raising the transmitter, and a corresponding factor applying to the receiver. An appropriate example is given in *fig. 4*, where the field strength in microvolts per m is shown for a transmitter radiating 1 kilowatt on a 7-m wave length and taking earth constants of $\sigma_{\mathrm{EMU}} = 10^{-13}$ and $\varepsilon = 4$

---

[3] The form of this equation has been adapted to the equation already derived by one of the present authors (Balth. van der Pol Hochfrequenztechn. **37**, 152, 1931) for a flat earth. In this case, instead of (1), we get

$$E_{\mathrm{mV/m}} = \frac{300\ \sqrt{P_{\mathrm{kW}}}}{D_{\mathrm{km}}} \cdot f(\varrho), \quad . \quad . \quad . \quad . \quad (1^*)$$

where the "numerical distance" is given by the expressions:

$$\left.\begin{aligned} \varrho &= \frac{\pi \cdot 10^{-9}\ D_{\mathrm{km}}}{6\ \sigma_{\mathrm{EMU}}\ \lambda_{\mathrm{m}}^{2}} \\ \text{and} \qquad f(\varrho) &= \frac{2 + 0.3\,\varrho}{2 + \varrho + 0.6\,\varrho^2} \end{aligned}\right\} \quad . \quad . \quad . \quad . \quad (1^{**})$$

(corresponding to an average soil), and the ideal case for σ = infinity. This curve was not calculated by means of the approximation formula, given in equation (1), but by strict expansions of series, which owing to their complexity have been omitted in this article. The curves $h_1 = 0$ refer to the transmitter and receiver both on ground level, and curves $h_1 = 100$ m to one station at a height of 100 m. with the other again at ground level. According to a general principle, the same field strength is obtained if the positions of the transmitter and receiver are interchanged; so that it is immaterial here whether the transmitter or the receiver is assumed to be raised to 100 m.

This figure brings out clearly three general characteristics regarding the propagation of electric waves:

1) *The occurrence of the height-gain factor,* which means that for long distances D the ratio of the field for $h_1 = 100$ m and the field for $h_1 = 0$ is independent of the distance D, to a first approximation; in the fully calculated example given here this ratio varies only within the narrow range of 25 and 35 for all distances of D_{km} greater than 2.
2) *The effect of the earth's resistance.* The field strengths, which would be obtained with the same 1-kilowatt transmitter and the same wave length of 7 m if the earth possessed infinite conductivity or were a perfect reflector, are given at the top of the graph. Here again, we have plotted the curves next to one another for transmitter and receiver both at ground level ($h_1 = 0$) and for one station at a height of 100 m ($h_1 = 100$ m). It is apparent that the gain in field strength by raising the receiver or transmitter is much less marked in this case, although the field strengths itself have become much greater. This can be explained by the fact that now, the earth's absorption being absent, it cannot be diminished by raising the sender. Therefore this has only the effect of reducing reflection losses which, as already pointed out, are generally much smaller.
3) *The horizon effect:* the curves for $h_1 = 100$ m are continuous up to the point $D_{\text{km}} = 35.7$, *i.e.* the point where the optical horizon of the transmitter is intercepted. Thus with these ultra-short waves no sudden and marked reduction in the field strength occurs at all, if the receiver is located below the optical horizon of the transmitter, *i.e.* no marked shadow effect is produced by the earth. It must be remembered that even the shortest waves used in wireless are still very long as compared to optical wave lengths, which naturally produce a pronounced shadow effect. Theoretically, in the optical case the precise shadow effect can be deduced by adding a sufficient number of terms in the neighbourhood of the optical horizon to the series obtained on transformation of the original series of spherical functions; equation (1) which corresponds to the first term of this series will then no longer represent a satisfactory approximation.

To bring out clearly that a pronounced shadow effect would indeed be obtained with waves of the order of 1 cm, the factor E/E_{pr} has been plotted in *fig.* 5 as a function of the distance D for an earth of perfect conductivity, again assuming the transmitter to be at a height of 100 m; this factor expresses how many times the field strength E_{pr} of a transmitter located in the open is increased or diminished by the presence of the earth. In the immediate neighbourhood of the transmitter this ratio is 2, as the interaction of the direct waves and those reflected by the earth doubles the field strength. Where a marked shadow effect is obtained, the curves behind the point on the horizon at $D_{\text{km}} = 35.7$ should diminish very abruptly and considerably, but this is seen not to be the case for wave lengths

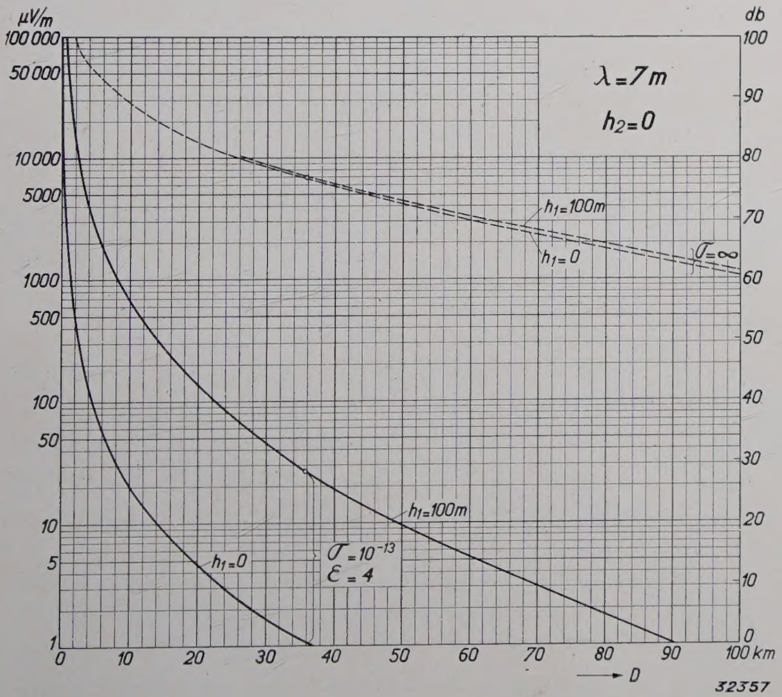

Fig. 4. Field strength surrounding a transmitter over the earth's surface as a function of the distance, for a 1-kilowatt transmitter radiating on a wave length of 7 m. h_1 is the height of the transmitter above the surface, and σ and ε are the conductivity and dielectric constant of the soil respectively.

of 7 m and 0.7 m as used in radio transmission. For still shorter waves, the field is indeed cut off very sharply beyond the horizon, as shown in the figure, and it then exhibits a behaviour as normally found with optical waves. If the finite conductivity of the earth were taken into consideration, the shadow effect would become less marked owing to the intervention of other similar phenomena resulting from the absorption due to the earth. On the other hand, the shadow effect becomes sharper if transmitter and receiver are both raised above ground level, as may be also gathered from a comparison of *figs. 7* and *8*. First consideration will, however, be given to the field strength in front of the horizon.

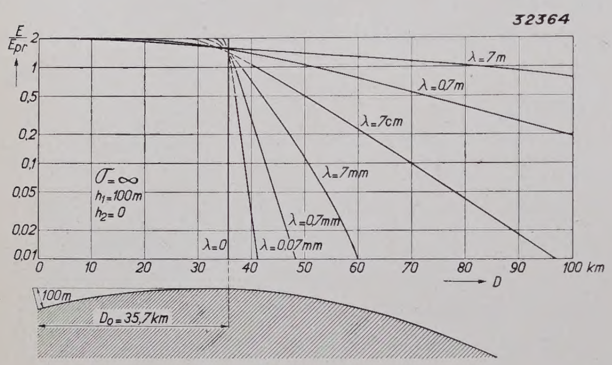

Fig. 5. Ratio of the field strength E at the surface to the field strength E_{pr}, which would obtain in the absence of the earth, plotted for various wave lengths as a function of the distance D from the transmitter. In the case under consideration with a transmitter at a height of 100 m and assuming infinite conductivity of the soil, a shadow boundary (horizon) only becomes apparent at wave lengths less than several millimetres.

Evaluation of the Field Strength at Short Distances from the Transmitter (In front of and beyond the Horizon)

The propagation of wireless waves can be analysed by similar principles to those employed with light waves, for which very good approximations are given by geometrical optics assuming the rectilinear propagation of light rays, provided points close to or in the shadow of the light source are left out of consideration. Very close to the transmitting station, *i.e.* a long way in front of the optical horizon, the field strength may be regarded as compounded from a ray ZP (*fig. 6*) travelling directly from the transmitter Z to the point of reception P, and a ray ZTP which in its travel has been reflected once at a point T on the earth's surface. In reality rays also penetrate the earth at T, but these are very rapidly absorbed and can, therefore, be neglected (*cf.* fig. 2).

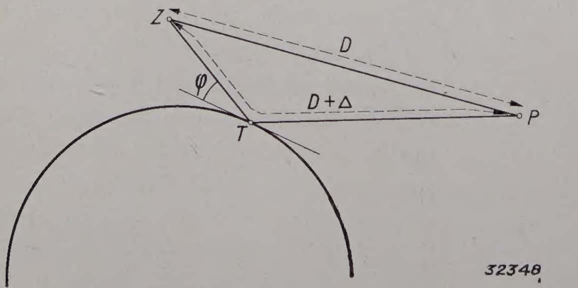

Fig. 6. The field strength at the point P due to the transmitter Z is created by the direct wave and by a wave which is reflected at T on the earth's surface.

In the geometric-optical approximation, the field strength due to the reflected wave should be added to that due to the direct wave, but the former arrives at P with a displacement in phase relative to the direct wave, since it has to traverse a distance which is longer than that of the direct wave by the amount $ZT + TP - ZP = \Delta$. In addition its intensity is reduced by reflexion and has to be multiplied by the usually complex coefficient of reflexion R; hence the ratio of the field strength in the presence of the earth to that in its absence is given by the expression:

$$\frac{E}{E_{pr}} = \left| 1 + R \cdot e^{2\pi i \Delta/\lambda} \right| \quad . \quad . \quad . \quad . \quad (3)$$

The complex coefficient of reflexion R occurring in this expression depends on the magnitude of the angle of incidence φ which the wireless wave makes with the earth's surface, and also on the electric constants of the earth. On displacing point P the position of T is also altered, as well as the value of φ and hence the coefficient of reflexion. If the receiver is not too close to the transmitter, φ will be very small and a coefficient of reflexion corresponding to grazing incidence ($\varphi = 0$) can be assumed; furthermore, the strong absorption of the earth allows R to be put approximately equal to -1, *i.e.* the earth reverses the phase of the incident wave (note that, on the other hand, with a perfectly reflecting earth, $R = +1$).

This analysis, however, cannot allow for the spherical shape of the earth. But, on starting from the original series of spherical harmonics, the geometric-optical approximation can be regained by applying another transformation other than that used for long distances, (*viz.*, a multidimensional application of the method of steepest descent), and thus the influence of the curvature of the earth can be calculated. One obtains the following results:

1) Owing to the spherical shape of the earth the reflexion coefficient R is altered slightly to a new value R', and

2) The strength of the reflected wave must be further multiplied by a supplementary factor δ, the divergence factor. This factor has a value less

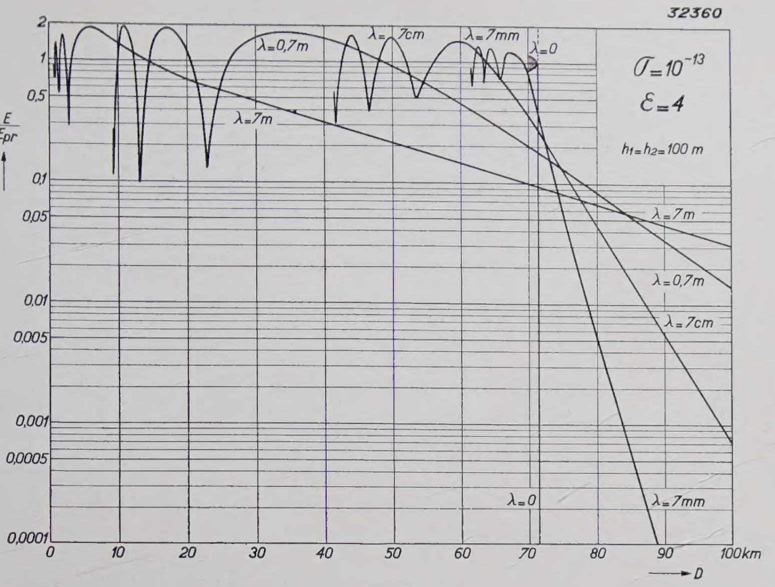

Fig. 7. Ratio of the field strength E along a line drawn through the transmitter parallel to the earth's surface, to the field intensity E_{pr} which would obtain in the absence of the earth. The wavy nature of the curve is due to interference between the direct and reflected waves. With waves below 1 cm, the effect of the optical horizon is clearly apparent. The curves are for average electrical properties of ordinary soil ($\sigma_{\mathrm{EMU}} = 10^{-13}$, $\varepsilon = 4$).

than unity and accounts for the increase in dispersion after reflexion of a small pencil of rays reflected by a spherical earth as compared with a pencil reflected at the same point on a flat earth; the divergence factor is thus a pure geometrical magnitude and does not depend on the wave length or the electrical characteristics of the earth. The geometric-optical approximation corrected in this way hence assumes the following form in place of (3):

$$\frac{E}{E_{pr}} = \left| 1 + \delta \cdot R' \, e^{2\pi i \Delta/\lambda} \right| \quad . \quad . \quad (4)$$

If both transmitter and receiver are at ground level, this additional divergence of the reflected wave does not occur and δ must then be taken as unity.

Entirely new phenomena appear when both the transmitter and receiver are raised above the earth's surface, for then interference between the waves can take place since the direct and the reflected waves can arrive at the point of reception in phase or with opposing phases; in this case they either partially reinforce or weaken each other. If the effect of divergence is neglected, as is frequently done in elementary analysis of the problem, and the coefficient of reflection is taken as —1, interference maxima are obtained at points where $\Delta = {}^1/_2\,\lambda$, ${}^3/_2\,\lambda$, ..., and minima where $\Delta = \lambda$, 2λ, ... the field strength would then be zero at the minima. Since the coefficient of reflexion is not exactly —1, and since the divergence factor is less than unity, the direct and the reflected waves never completely cancel each other out, (not even if the geometric-optical approximation given above represented a strict expression of the field strength). The cumulative effect of the two phenomena is that, on the one hand, the maxima and minima are less pronounced and, on the other, that they are slightly displaced in position.

As a special case, we may take the transmitter and receiver as raised to the same fixed height above the earth's surface, and then study the field strength as a function of their distance apart. If the receiver is located close to or beyond the horizon, the series must be taken in which the first term is given by equation (1); in the range before the shadow region a gradual transition is found from this series into the geometric-optical formula 5a, and for still shorter distances computations can be made with the equation. The authors have performed this computation for a height of 100 m for both transmitter and receiver and for earth constants of $\sigma_{\mathrm{EMU}} = 10^{-13}$ and $\varepsilon = 4$, corresponding to average soil. In *fig.* 7 the values for the ratio E/E_{pr} have been plotted for various wave lengths, the maximum value of this ratio being 2 as already indicated (assuming the earth as flat and

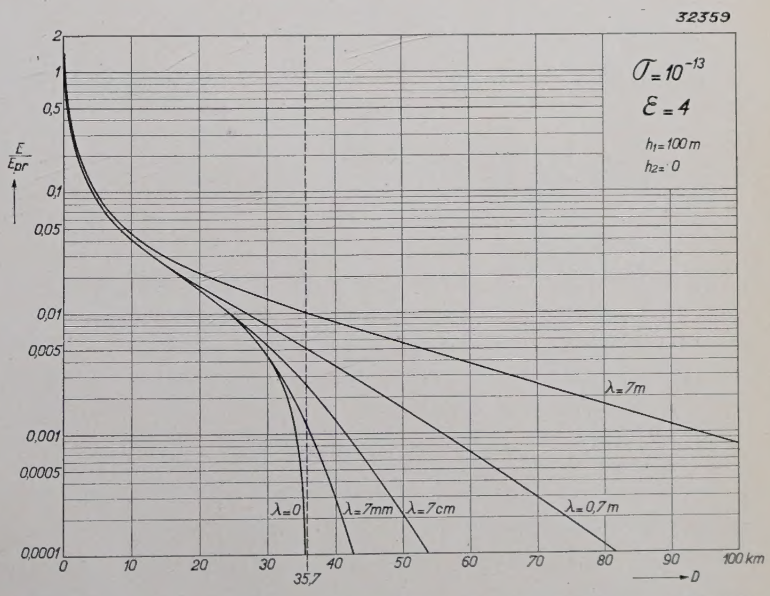

Fig. 8. Ratio E/E_{pr} over the earth's surface with the transmitter at a height of h_1 = 100 m for an ordinary soil ($\sigma_{\mathrm{EMU}} = 4 \cdot 10^{-13}$, $\varepsilon = 80$) for distances up to 2 000 km for a radiated output of 1 kilowatt.

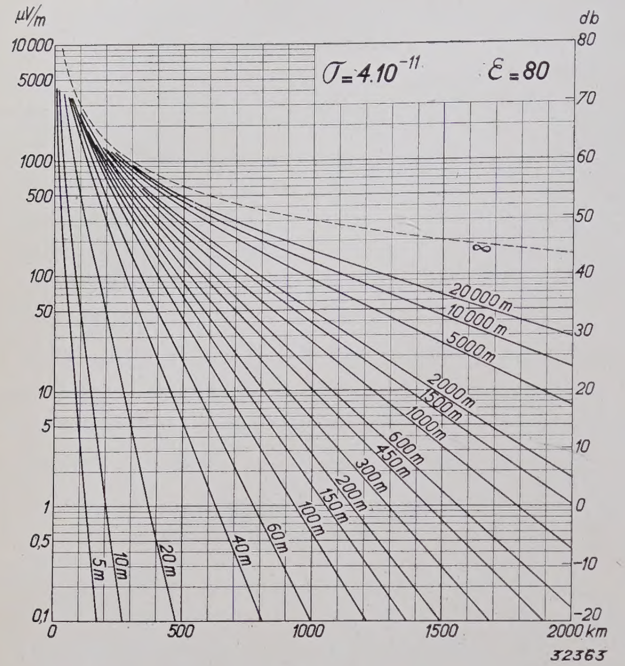

Fig. 9. Field strength of a transmitter above sea level ($\sigma_{\text{EMU}} = 4 \cdot 10^{-11}$, $\varepsilon = 80$) for distances up to 2 000 km with a radiated output of 1 kilowatt (transmitter at sea level).

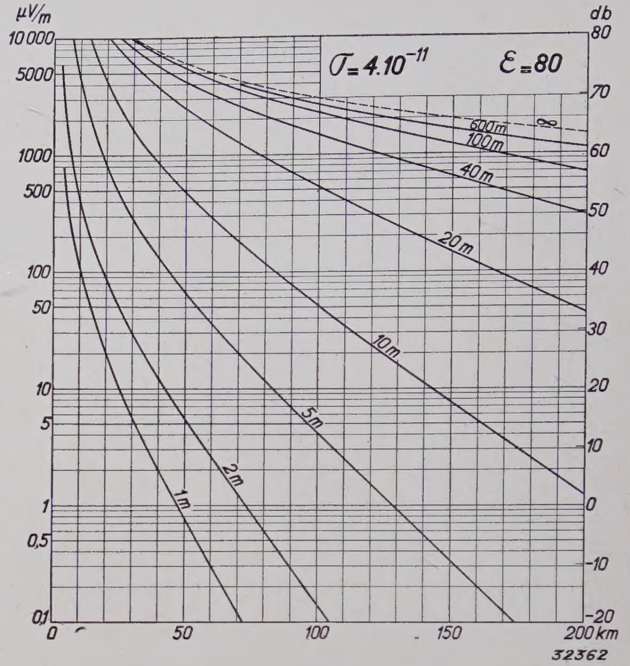

Fig. 10. The same as fig. 9, but drawn on a larger scale for distances up to 200 km.

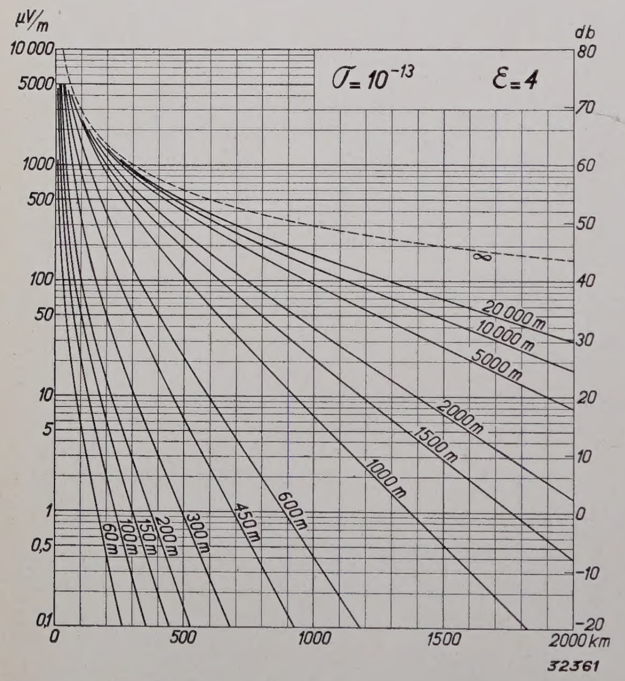

Fig. 11. Field strength of a transmitter on the surface with an average soil ($\sigma_{\text{EMU}} = 10^{-13}$, $\varepsilon = 4$) for distances up to 2 000 km with a radiated output of 1 kilowatt.

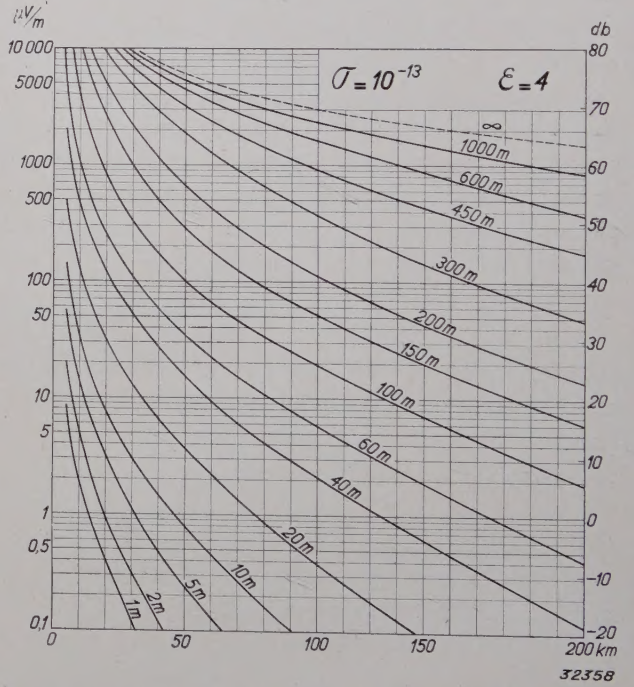

Fig. 12. The same as Fig. 10, but on a larger scale for distances up to 200 km.

giving specular reflection). This graphical representation clearly shows interference maxima and minima in the region in front of the optical horizon, which is now located at a distance of 2 × 35.7 = 71.4 km as both transmitter and receiver are at elevations of 100 m. It is seen again here that, contrary to many assertions, there is no question of a sharp shading on passing through the optical horizon, even with the shortest wireless waves used. The rapid diminution of the field strength beyond the horizon appears to commence already in front of the horizon, in fact at the last interference maximum, *i.e.* the maximum nearest to the horizon, while the slope of the curve changes only very slightly on entering the shadow region. This last-named maximum will be the closer to the horizon, the shorter the wavelength; in the limiting case of zero wave length the field would disappear at the horizon.

Finally, *fig. 8* shows for the same electric constants of the earth and the same wave lengths the corresponding curves with the transmitter at a height of 100 mm. and the receiver on ground level. In this case, interference phenomena naturally do not occur, since the direct and the reflected waves arrive at the point of reception without any difference in phase. This graph represents the same function as fig. 5 which, however, has been calculated for infinite conductivity.

General Results with both Transmitter and Receiver at Ground Level *(complete wave range and distances up to 2 000 km)*

The field strengths were calculated as a function of the distance D for 19 different wave lengths between 1 m and 20 000 m, for propagation over the water (electrical constants: $\varepsilon = 80$ and $\sigma_{\mathrm{EMU}} = 4 \cdot 10^{-11}$). The curves were calculated using different series expansions for different distances. *Figs. 9, 10, 11* and *12* give the field strengths expressed in micro-volts per m for a transmitter radiating 1 kilowatt. Figs. 9 and 11 give the field strengths up to the distances of 2 000 km from the transmitter, while figs. 10 and 12 show on a larger scale the field strengths up to distances of 200 km only. The broken line at the top of the graphs represents the field strength which would be obtained with the earth flat and exhibiting specular reflection.

These graphs show clearly that particularly with shorter waves the field strength diminishes much more rapidly in propagation overland than in propagation over water, a result mainly due to the fact that in the former case the waves are much more strongly absorbed during their travel. As already pointed out, the effect of this absorption is usually much greater than that due to the curvature of the earth. The higher the conductivity of the soil the lower will this absorption be as a rule, and hence the greater the field strength, other conditions being equal. An exception to this rule is obtained only when very long waves travel over considerable distances, and where propagation may suffer slightly with a higher conductivity. It may be seen from figs. 8 and 10 that *e.g.* for $D = 2\,000$ km the field strength at $\lambda = 20$ km in propagation over land is 4 per cent greater than in propagation over water. In general, for a given wave length, there is a specific value of conductivity which gives the optimum propagation over long distances and which is given by the equation:

$$\sigma_{\mathrm{EMU}} = \frac{2.25 \cdot 10^{-7}}{\lambda_{\mathrm{m}}^{5/3}} .$$

Both with constant wave length and distance, the field strength is reduced if the conductivity is made smaller or larger than this value, but this maximum field strength is by no means sharply defined. Where the wave length is not too great, the conductivity values actually obtaining are usually below this value and hence an improvement in propagation would result if the conductivity of the soil could be enhanced.

In conclusion, it should be emphasised that, although fairly extensive simplifications have been introduced in all calculations made here, experimental measurements of the field strength are in the majority of practical cases in agreement, at least as regards order of magnitude, with the theoretical results set out above.

BIBLIOGRAPHY

In addition to the papers contributed by the authors, computations of the propagation of wireless waves round the curved surface of the earth have also been published recently in the following papers:

Eckersley and Millington, Proc. Roy. Soc., London, A **136**, 499, 1932; Phil. Trans. **237**, 273, 1938; Phil. Mag. **27**, 517, 1939.

Wwedensky, Techn. Phys. U.S.S.R., **2**, 624, 1935; **3**, 915, 1936, and **4**, 579, 1937.

A survey of theoretical principles and experimental data covering the whole field of wireless wave propagation is also given in the Report of the Committee on Radio-Wave Propagation, issued by the International Consultative Committee for Radio Communication (C.C.I.R.), which has also been published in Proc. Inst. Rad. Eng., **26**, 1193, 1938.

PRESSURE CONDENSERS

by C. de LANGE.

621.319.46

In alternating-current condensers with a dielectric of oil-impregnated paper, the permissible field strength can be increased by applying a pressure to the oil, thus raising the reactive power per unit of volume which the condenser can absorb. The effect of increasing the pressure is explained and the construction of pressure condensers is discussed in this article.

In a previous article in this Review [1]), an outline was given of the construction of heavy-current condensers, which are used principally for improving the power factor in alternating-current systems. These condensers are made up of reels composed of aluminium foil with intermediate layers of thin paper. The maximum voltage V which can be impressed on the reels depends on the thickness d of the dielectric, for V/d must not exceed the maximum field strength permissible with the particular dielectric used. For a given volume of reel the thickness d of the dielectric also determines the capacity C. With an alternating current of angular frequency ω the reel can absorb a reactive power of:

$$W = V^2 \omega C \quad . \quad . \quad . \quad . \quad . \quad . \quad (1)$$

In practical designs of these condensers, reels are made with a dielectric of 20 to 60 μ thickness, a capacity of 1 to 2 μF and a power rating W of some tens of VA.

The greater the reactive power to be taken up the more important does it become to increase the power rating W per reel to a maximum value, in order to make do with a reasonable number of reels, *i.e.* to arrive at a battery of condensers of reasonable size and which does not occupy too much space. An increase of W in a reel of given dimensions may be obtained for a given dielectric constant by raising the permissible field-strength of the dielectric; for, with the same thickness of dielectric (capacity C), this will increase the permissible voltage V and in accordance with equation (1) give a quadratic increase in W.

In paper-insulated condensers working in an alternating-voltage system, as increase in the permissible field strength, which is normally about 10 volts per μ, can be obtained by placing the whole condenser under pressure. This method is discussed below, together with a short description of "pressure condensers" which have been designed on this principle.

Limitation of the permissible field strength

Paper is not a homogeneous material but a complex conglomeration of fibres separated by innumerable microscopic spaces and grooves. In the ordinary state the fibres enclose considerable quantities of air and moisture in these many cavities, which before using the paper in the manufacture of condensers must be carefully removed. This is necessary as the oxygen in the air may attack the "coatings" of the condenser as well as other components, while the moisture adversely affects the insulation and causes dielectric losses, apart from giving rise to the production of gases by electrolysis. The air and moisture are removed by a thorough degassing of the paper *in vacuo*, after which the paper is impregnated, *i.e.* the cavities are filled with a suitable material, in our case with oil.

In spite of this thorough pre-treatment, gas residues are still left in cavities of the dielectric, with the result that the maximum permissible field strength in the dielectric cannot be determined directly from the disruptive voltage of the paper fibres or from that of the oil. For this field strength depends on the weakest places in the dielectric, and in the gas inclusions undesirable phenomena, such as ionisation and electrical breakdown, may occur in the cavities at voltages which are much lower than necessary to produce similar effects in other parts of the dielectric. These reactions produce local overheating, which may result in carbonisation, the dielectric becoming progressively weaker until complete breakdown of the insulation occurs [2]). It is essential, therefore, to keep the field strength at a safe low value in order to avoid these undesirable phenomena.

Effect of Pressure

The field strength at which breakdown occurs in a mass of gas depends among others on the pressure of the gas. It has been found, however, that in a homogeneous field the disruptive voltage V_D is already determined by the product of the pressure p and the thickness h of the gas inclusion (thickness of cavity). The relationship between V_D and ph is represented by the Paschen curve shown in *fig. 1*. The curve has a minimum [3]) at which $V_D = V_I$; for air V_I = about 345 volts.

---

[1]) Philips techn. Rev. **1**, 178, 1936.

[2]) These considerations apply only to alternating-current loads. With direct-current loads, these phenomena are absent so that the permissible field strength is considerably higher.

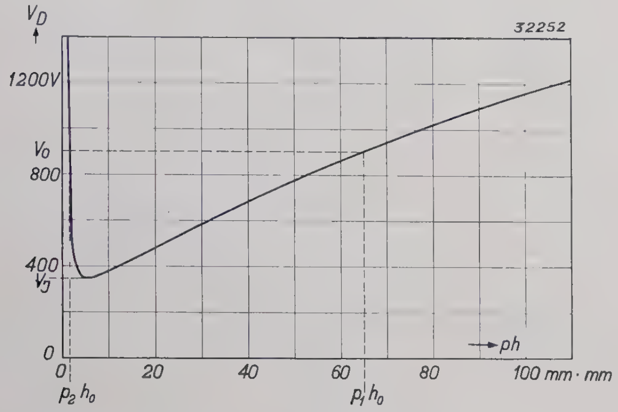

Fig. 1. Paschen curve for air (practically the same curve applies to nitrogen). This curve gives the relationship between the disruptive voltage V_D and the product ph of the pressure p and the distance h between the electrodes (thickness of cavity). For a given value h_0 and a voltage $V_0 > V_I$ breakdown occurs if the pressure is between p_1 and p_2.

At voltages below V_I, breakdown cannot occur at whatever value of ph, but if the voltage rises above V_I breakdown may take place at any pressure between two different pressures p_1 and p_2, assuming a constant thickness of layer h_0 (see fig. 1). This breakdown may be avoided, for that particular voltage and layer thickness, by reducing the pressure of the gas below p_2 or making it greater than p_1. In this way the permissible field strength at the gas inclusions and hence in the whole of the dielectric can be raised.

The first method, that of reducing the pressure sufficiently low, is not feasible in practice, as it cannot be ensured that no gas inclusions remain which are at a higher and hence dangerous pressure. The second method is, therefore, adopted and a high pressure applied in order to avoid a breakdown occurring in any and every gas-filled cavity. That portion of the Paschen curve to the left of the minimum can be neglected in what follows.

Determination of the required pressure

Take a specific case in which the voltage V applied to the condenser reel and the thickness d of the dielectric are known. The thickness h of any gas layer occluded in a cavity of the dielectric may vary between 0 and d. The pressure must therefore be made so high that for every cavity $0 < h < d$ the disruptive voltage V_D will be greater than the voltage V_h impressed on the cavity.

As the maximum possible voltage $V_h = V$ is impressed on a cavity which occupies the whole space between the coatings of the condenser ($h = d$), one might be inclined to assume that this cavity is most susceptible to a breakdown, *i.e.* the greatest pressure would be necessitated by this case. It is found, however, that for a cavity of thickness $h_m < d$ the pressure required to prevent breakdown has a maximum value. This maximum may be determined as follows:

At the boundary between the dielectric and a cavity the field strength changes abruptly, because the dielectric constant ε is not the same on both sides of this surface. In the paper $\varepsilon = \varepsilon_p$, for which we may take the value 4.2, while in the gas inclusion $\varepsilon = 1$. The potential distribution can be readily calculated with the aid of *fig. 2*. The two components with thicknesses d—h and h respectively are regarded as two condensers in series with capacities C_p (:) $\varepsilon_p/(d - h)$ and C_h (:) $1/h$ respectively. Since the same displacement current must flow for both condensers, we have:

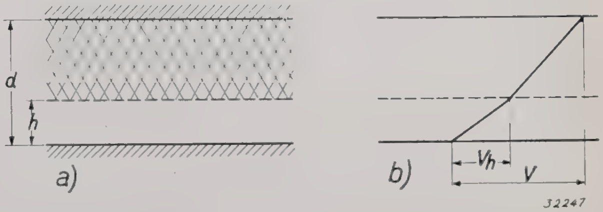

Fig. 2. *a*) To calculate the voltage V_h which, at a voltage V between the coatings of the condenser and a thickness d of the total dielectric, is impressed on a cavity of thickness h in the dielectric, the parts of the dielectric filled respectively with paper and gas are regarded as two condensers in series.
b) At the boundary surface the potential between the coatings shows a sharp change (the field strength changes abruptly).

$$(V - V_h)\,\frac{\varepsilon_p}{d-h} = V_h\,\frac{1}{h},$$

hence:

$$V_h/V = \frac{\varepsilon_p \cdot h/d}{1 + (\varepsilon_p - 1)\,h/d} \quad . \; . \; . \quad (2)$$

In *fig. 3*, the ratio V_h/V is plotted as a function of the ratio h/d. If concrete values for a particular case are taken for the parameters V and d, the curve representing V_h as a function of h can be derived from *fig. 3* by altering the scales along the coordinate axes. This curve can then be combined with the Paschen curve in fig. 1 and for every thickness of cavity h, the minimum value of ph can be found for which the disruptive voltage V_D is greater than the impressed voltage V_h. The required pressure p_1 then follows from h and the value of $(ph)_1$ thus found. In *fig. 4* the value of p_1 found in this way is plotted as a function of h for $d = 30$ μ and for different values of V (crest value of alternating voltage). It is stated that each of the curves passes through a maximum. The curve for $V = 800$ volts, *e.g.*, has a maximum at $h_m = 9.6$, where p_1 has a value of $p_{1m} = 2\,520$ mm Hg or 3.45 atm. If, therefore, the pressure is made greater than 3.5 atm., then in the case under consideration with $d = 30$ μ and $V = 800$ volts neither ionisation nor breakdown can occur in any cavity which might be present in the dielectric.

---

[3]) For the explanation of the increase of V_D with decreasing ph, in the left part of the curve, *cf.* this Review **1**, 10, 1936 or **3**, 333, 1938.

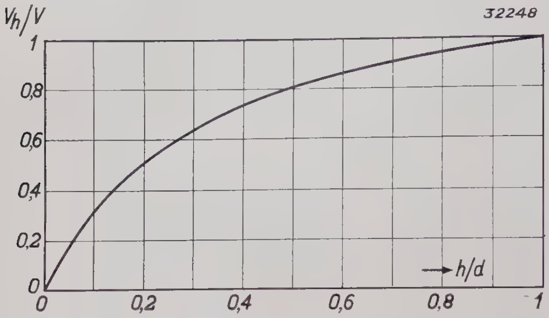

Fig. 3. The ratio of the voltages V_h/V plotted as a function of the ratio h/d. The curve shows V_h as a function of h, if the axes are scaled in terms of the parameters V and d.

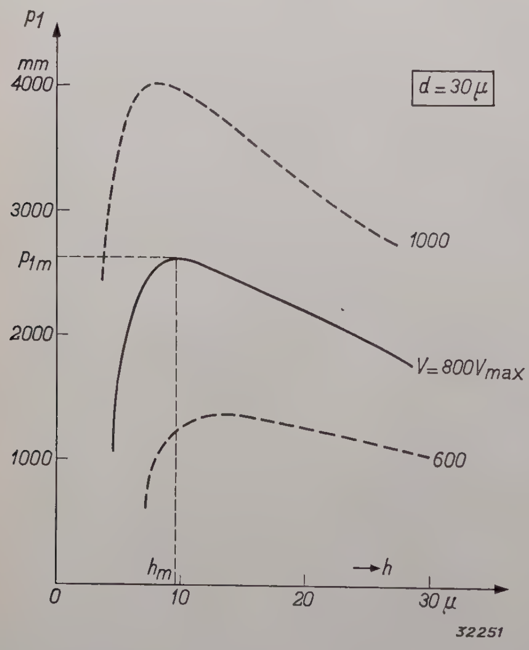

Fig. 4. By applying the equality $V_h = V_D$ the curves in fig. 1 and fig. 3 give the pressure p_1 required with different cavities (h) in order to prevent breakdown. This pressure is plotted here for $d = 30$ μ and different values of V as a function of h. In each curve for a certain value of $h = h_m$, p_1 has a maximum value p_{1m}.

If for a given value of d (*e.g.* 30 μ) the required pressure p_{1m} is plotted as a function of V, a curve of the type shown in *fig. 5* is obtained, which shows how high the pressure must be made to allow a condenser reel with that particular thickness of dielectric to sustain safely an impressed voltage V. For other values of the thickness d, the required pressure follows directly from the fact that for a given value of V the product of $p_{1m} \cdot d$ is constant. The figure reproduces the curves for four different values of thickness of dielectric.

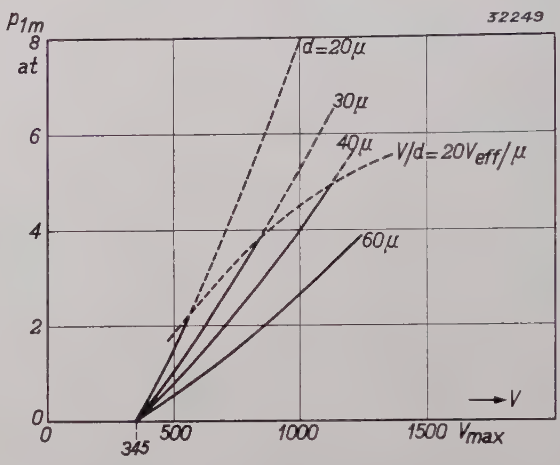

Fig. 5. The required pressure p_{1m} plotted as a function of the voltage V (effective value) between the coatings, for different thicknesses d of the dielectric. The parts shown by broken lines do not enter into practical consideration, as here the field strength of 20 V_{eff}/μ (see below) is exceeded.

Pressure differences in the dielectric

In practice, the required increased pressure is obtained by immersing the condenser reel in oil in a suitable casing and applying a pressure to the oil. This does not, however, ensure that the same pressure will be obtained in every cavity present in the dielectric; this equality would only occur if an equilibrium were established, which, however, is continually disturbed while the condenser is in service. The temperature of the condenser varies owing to the heat evolved as a result of dielectric losses, and the paper and oil in the dielectric expand not entirely uniformly, so that local pressure gradients may arise which are only removed again when the oil has had a chance to flow into any low-pressure area created. To ensure that this flow takes place as quickly as possible, an oil must be selected which has a sufficiently low viscosity, even at the lowest temperatures likely to occur in practice. Furthermore the paper ought to be to the highest possible degree permeable to the oil. But this is in opposition to the need for realising as high a dielectric constant and disruptive voltage in the dielectric as possible. Satisfactory permeability demands a low filling factor for the paper, *i.e.* a loose fibrous structure fitted with a large number of pores, while for a high disruptive voltage and a high average dielectric constant the filling factor must be high[4]).

This difficulty is avoided by dissolving in the oil a gas, such as nitrogen, which will not attack the coatings of the condenser of the dielectric. The quantity of gas dissolved depends to a large extent on the pressure in the liquid. Should the pressure fall in a cavity owing to delay in the oil flow, nitrogen is then immediately liberated in the cavity which it fills temporarily, becoming dissolved again as oil flows back into the cavity.

Nevertheless, in every case, it is essential to make the pressure applied externally much greater than the value derived theoretically, so as to maintain a sufficient pressure in all cavities, even during a temporary local fall in pressure.

If a breakdown due to ionisation in the gas inclusion is completely inhibited by this means, the field strength in the dielectric can be increased and will no longer be determined by the cavities, but now *e.g.* by the properties of the oil. This field strength is found by experiment, measurements having shown that in practical cases where the pressure has been raised to between 8 and 15 atm. the maximum permissible field strength in the dielectric could be roughly doubled, *e.g.* about 20 volts per μ (this limitation is also indicated in *fig.* 5). This result signifies that by the application of pressure the voltage impressed on a condenser reel can be doubled, so that only a quarter of the number of reels are required to obtain the same capacity than when no pressure is applied. In practice this potential improvement is not entirely utilised, a portion being reserved for increasing the safety factor.

Construction of pressure condensers

The manner in which a pressure is applied to the dielectric has already been indicated above; the pressure is impressed on a totally-enclosed mass of oil which surrounds the batch of condenser reels. This principle can be translated into practice in various ways. Thus the pressure can be communicated to the oil over a diaphragm. In this case, however, the oil must be given facilities for expansion on fluctuations in temperature. The casing has then to be fitted with an expansion unit, which will make the general design much more complicated. Another method was therefore adopted in Philips pressure condensers; only part of the condenser tank is filled with oil and the space above the oil filled with compressed nitrogen; this method also provides for the requisite solution of the nitrogen in the oil. A few details of general interest regarding the construction of these condensers are given here.

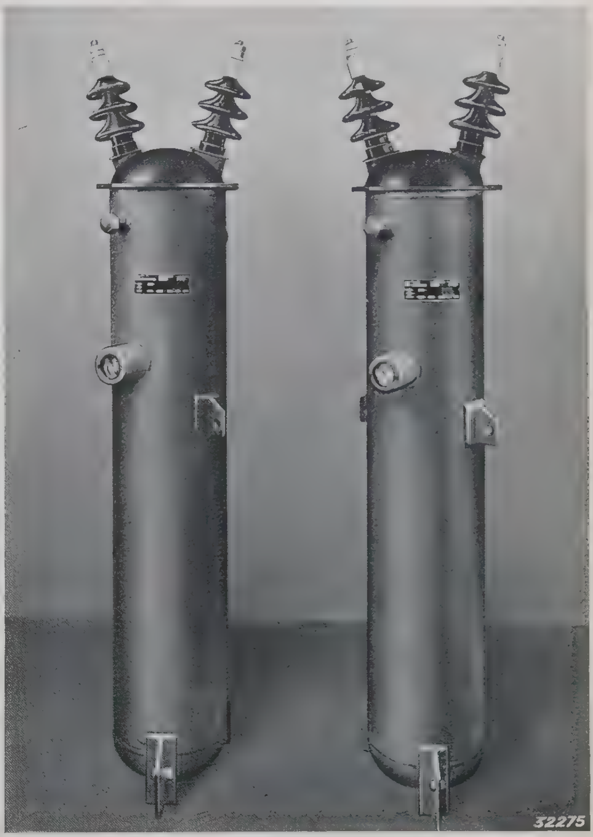

Fig. 6. Pressure condensers for 50 kVA and a working voltage of 10 000 volts effective, two-phase, 50 cycles. The condenser reels are enclosed in a seamless steel tube, a manometer being inserted at half the height of the condenser to measure the pressure. The initial pressure is here about 20 atm. Just above the pressure gauge is the pressure release, which is protected on the outside by a nut.

The tank or casing enclosing the condenser reels is a seamless steel tube to which a base and a cap are welded (*fig. 6*). This longitudinal shape facilitates the dissipation of the heat evolved in the condenser, since a large surface per unit of volume is provided (this ratio is a minimum with a sphere). The gastightness of the tube and particularly of the glands through which the electrodes are passed and the various connections must naturally satisfy severe specifications. The general standard of gastightness adopted is that the pressure must be maintained above the minimum value of 8 atm. over a period of three years. All connections on the tube are, therefore, welded or soldered and carefully tested for leakage.

---

[4]) The fibres have a dielectric constant of approximately 6, while the mineral oil used for impregnation (filling of the pores) in Philips' condensers has a dielectric constant of about 2 only. Synthetic oils for impregnation which have a higher dielectric constant are available, and therefore allow a lower filling factor to be realised. But these oils have the undesirable property that they attack the skin, a danger which is avoided by using mineral oil.

The life of the condenser reels is practically unlimited, thus a condenser becomes equivalent to new if nitrogen is recharged at regular intervals. filling and recharging of gas are done through a rubber valve, similar to that used on motor-car tyres. A valve of this type is naturally unsuitable as a seal; moreover the rubber is attacked by the oil. A reliable seal is, therefore, obtained with a cap which, after charging the condenser with gas, is placed over the valve and soldered. To recharge, the seal is unsoldered and the valve disc which has become useless in the meantime is then renewed.

As the temperature of the condenser rises, the pressure also increases; the maximum increase in pressure found in practice is 20 per cent (with a temperature rise of about 40 deg.), which can be withstood by the condenser tank in perfect safety. Of course, precautions are taken to deal with any excessive increase in pressure which might be created when electrical damages in the condenser occur, for instance as a consequence of surges. A thin copper diaphragm has been welded in the side of the tube close to the cap to provide a release at pressures below 100 atm. As the glands fail only when the pressure rises above 250 atmos. while the critical pressure of the tube is much higher still, this form of pressure release provides adequate protection. Similar to the precautions with oil-immersed transformers, a wide length of pipe may be mounted in front of the release disc so that any oil ejected when the diaphragm is ruptured can be collected in a suitable tank.

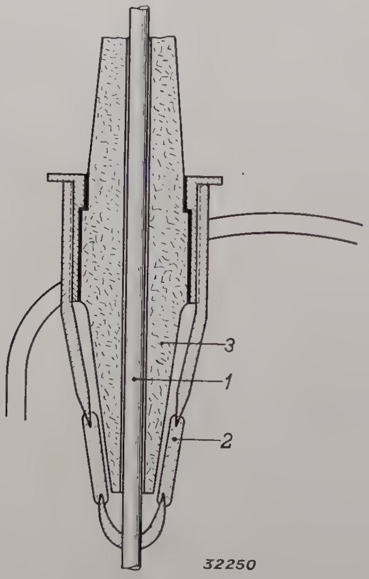

Fig. 7. Section of an electrode gland. The electrode stem *1* is fused into a glass insulator *2* with a chrome-steel liner, the glass insulator in its turn being welded into the cap of the condenser tube with a similar liner. On the outside, the electrode stem is supported by a ceramic insulator *3*.

The glands referred to above are shown in section in *fig. 7* and the glass insulators fixed inside the tube in *fig. 8*. The high compressive strength of 250 atm. for the glass insulators is obtained by very slowly cooling them after sealing into the tube, so that maximum stress relief is obtained. A gastight and heat-resisting seal between the glass and the electrode stems and the tank is obtained with the aid of chrome-steel liners. On the outside of the tank the electrode stem is supported by a ceramic insulator, in order to avoid torsional and bending stresses being communicated to the gland. A special point was made in the design of these insulators to provide complete protection for the glass in the event of an insulator breaking, as well as to enable the insulators to be renewed easily.

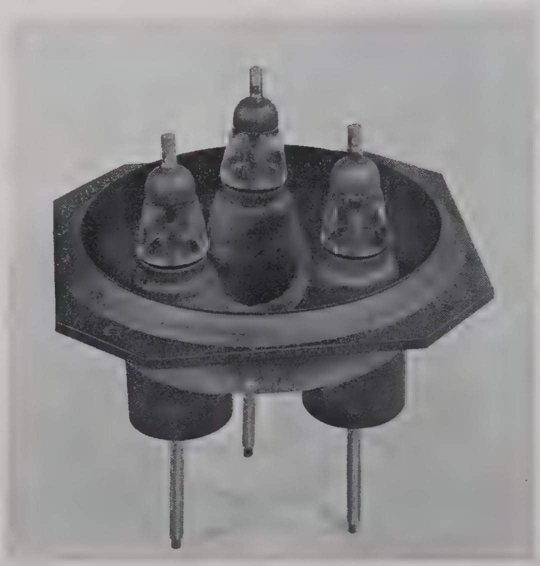

Fig. 8. Glass insulators of electrode glands in the cap of a three-phase condenser.

Pressure condensers are made for power ratings from 10 to 100 kVA and for effective voltages from 380 to 10 000 volts. No appreciable gain is realised by adopting a pressure design in condensers with ratings below 10 kVA, since the economy effected in the number of condenser plates does not make up for the complications by the high-pressure desing.

In fig. 6, two pressure condensers have already been shown, which are built for 50 kVA and 10 000 volts and which also are suitable for an open air mounting. Generally, pressure condensers may well be used in this kind of mounting owing to the entirely tight enclosure of the reels, the latter being thus protected against atmospheric influences.

A battery of pressure condensers, rated for a reactive power of 80 kVA each at a working voltage of 2 000 volts effective (three-phase, 50 cycles). is shown in *fig. 9*.

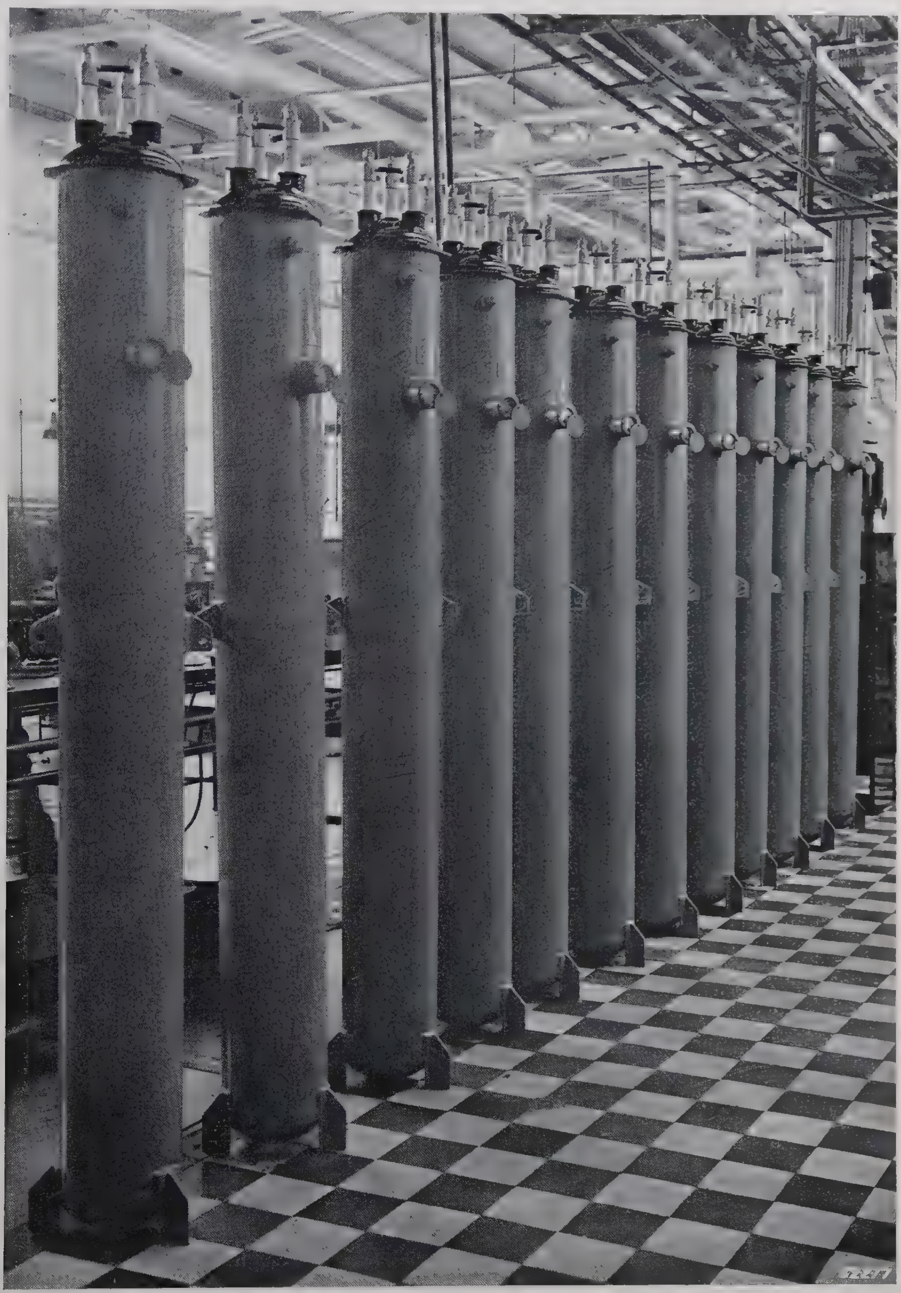

Fig. 9. Battery of pressure condensers rated for a reactive power of 1 000 kVA and a working voltage of 2 000 volts effective.

PHYSICAL PHOTOMETRY

by J. VOOGD.

535.247

This article discusses in how far it is possible to conduct photometric measurements entirely by physical means. The chief problem here lies in the accommodation of the spectral sensitivity of the apparatus to the international ocular sensitivity curve. This accommodation may be realised by using filters or by resolving the light into a spectrum and placing a suitable diaphragm in the path of the resolved rays. An analysis of the sensitivity and potential errors due to scattered light indicates that a combination of both methods offers the most satisfactory solution. A photometer developed in this Laboratory is described, with special reference to its calibration, accuracy and sensitivity.

The development of gas discharge lamps has brought the problem of heterochromic photometry to the forefront of interest. The fact that these lamps are selective radiators raises numerous knotty questions in visual photometry. A previous paper published in this Review has already called attention to these diffculties, and also gave an indication how they could be overcome by means of a physical photometer¹). The experience gained in the construction of a physical photometer in this laboratory is dealt with in the present article.

The basic problem in the application of photometry to a given source of light is to compare this source with a standard lamp which has itself been directly or indirectly calibrated against the light standard. All such comparisons must be carried out on the basis of the international luminosity curve; if, therefore, $E_1(\lambda)$ and $E_2(\lambda)$ are the energy fluxes which are emitted respectively by the light source under examination and by the standard lamp at the wave length λ per unit of wave band, per unit solid angle and per unit of time, a physical photometer must permit measurements, entirely by physical means, of the ratio of the candle powers as given by the expression:

$$\frac{I_1}{I_2} = \frac{\int E_1(\lambda)\, V(\lambda)\, \mathrm{d}\lambda}{\int E_2(\lambda)\, V(\lambda)\, \mathrm{d}\lambda}, \quad \ldots \quad (1)$$

where $V(\lambda)$ is the relative luminosity factor for the wave length λ. The physical photometer must carry out the integration occurring in equation (1), and in particular its spectral sensitivity curve must be identical with the international luminosity curve within narrow limits.

In the construction of a physical photometer, a receptor, *e.g.* a photo-electric cell, must be used, whose spectral sensitivity curve, of course, never will entirely coincide with the international luminosity curve. To obtain this correspondence, an accommodator must be placed in front of the receptor having an appropriate spectral transmission curve. This accommodation may be provided for in two ways:

1) Optical filters can be used, or

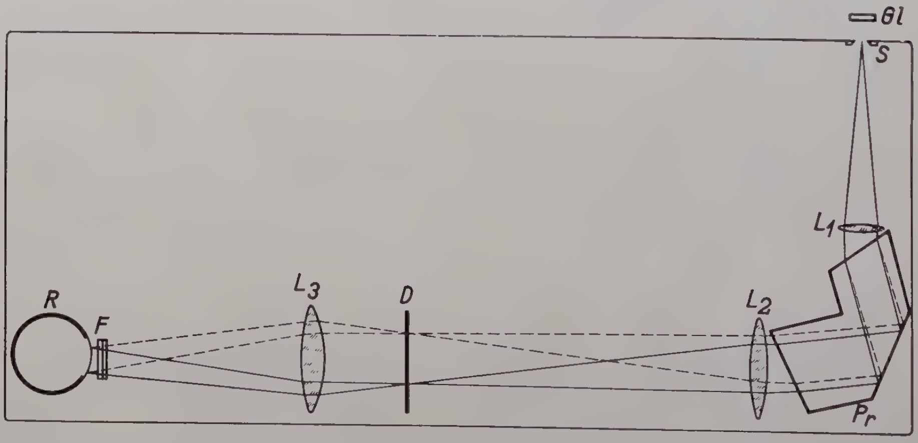

Fig. 1. Layout of a physical photometer. The light source whose candle power is to be measured, illuminates a depolished glass *Gl* in front of the slit *S*. A spectrum is produced from the light passing through the slit by means of the lenses L_1 and L_2 and the prism *Pr* and the spectrum is screened by the diaphragm *D* in such a way, that at every wave length the required fraction of the radiation is transmitted. An image of the collimator lens L_1 is projected by the lens L_3 through the filter *F* on the window of a photo-sensitive receptor *R*.

---

¹) Philips techn. Rev. **1**, 120, 1936.

2) The light before falling on the receptor can be resolved into a spectrum and the height of the spectrum can be lowered by means of a suitable diaphragm to the required fraction at each particular wave length.

Both methods have their own advantages and disadvantages. While optical filters provide a simple and sensitive apparatus if a rough correspondence is considered sufficient, great difficulties are encountered where the accommodation has to be rather exact. Spectral accommodation has the disadvantage that the sensitivity is low, for a spectrum must be produced and the only light available is the luminous flux which passes through the first slit on to the collimator lens (L_1 in *fig. 1*).

The limitation of the luminous flux conditioned by spectral adaptation becomes the more onerous, the more the spectral sensitivity curve of the receptor differs from the international luminosity curve. This will be analysed in greater detail.

An appropriate apparatus for the spectral adaptation is shown in fig. 1.

A depolished glass *Gl* is illuminated by the light source under investigation. Behind *Gl* is the slit *S* through which the light transmitted by *Gl* enters the apparatus. A spectrum is obtained by one of the usual methods, for instance by means of the two lenses L_1 and L_2 and a prism *Pr*. The diaphragm *D* is placed in the plane of this spectrum, and transmits the required fraction of the light of every wave length. The light is then concentrated by a lens L_3 on to a receptor *R*, in the present case a photo-electric cell. (The filter *F* shown in the diagram may be neglected for the moment).

Assume that a receptor has been chosen with a spectral sensitivity as given by line *a* in *fig. 2*. To obtain the international luminosity curve (line *b*), the screening produced by the diaphragm must vary with the wave length as indicated by line *c* in fig. 2. The form of this screening curve is most important, as it determines the maximum permissible width of slit and hence also the sensitivity of the photometer.

To comprehend this fact, consider the case where the width of the slit and the dispersion of the spectrum have been so chosen that the image of the slit when illuminated with monochromatic light subtends a constant wave band of 200 Å. The transmissibility for light with a wave length λ is then not determined by the height of the curve *c* at the point λ, but by the average value of curve *c* over a range from $\lambda - 100$ Å to $\lambda + 100$ Å. The error resulting herefrom will be the higher, the greater the curvature of line *c*. Conversely, for a given maximum error of *e.g.* 1 per cent, the width of the first slit and hence the sensitivity of the apparatus may be made the greater, the straighter the shape of the screening curve. In the example illustrated the transmissibility with a slit image of 200 Å width is 1 per cent too low at 5 800 Å, while at 5 000 Å it is 5 per cent too high. The slit should be about 2.5 times smaller in order to obtain an accuracy of 1 per cent at all points.

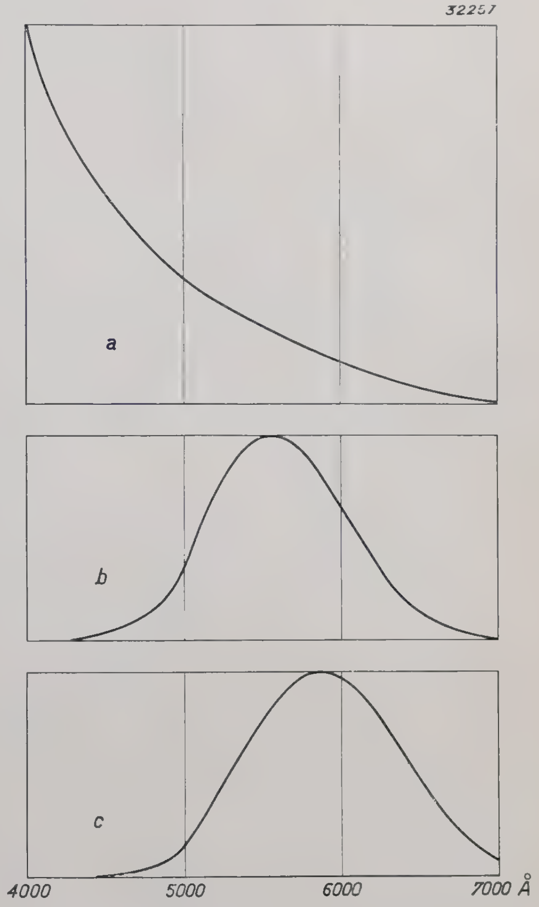

Fig. 2. *a*) Spectral sensitivity curve of a vacuum photo-cell with potassium cathode.
b) International ocular-sensitivity curve.
c) Transmission factor of a diaphragm which adapts the sensitivity curve of the photo-cell to the international ocular sensitivity curve, as a function of the wave length.

Apart from determining the maximum permissible width of the slit and hence the sensitivity of the photometer, the shape of curve *c* also determines in how far it is possible to eliminate errors resulting from the scattering of light in the optical system. Each point of the spectral plane receives not merely radiation of the corresponding wave length, but also a certain amount of scattered light, whose spectral composition may, to a first approximation, be assumed to be equal to that of the incident light. As a result of this, in addition to the fraction of each particular wave length of the light flux falling on L_1 which by normal optical means is projected on to the diaphragm (curve *c*), there is a certain constant percentage (in our photometer about 0.3 per cent) distributed over the whole diaphragm in the spectrum which is also transmitted.

The error, which results when the diaphragm is designed without taking this scattered light into consideration, will be the greater, the greater the variations of curve *c*. If the height of the diaphragm were the same for all wave lengths (*i.e.* were the diaphragm rectangular in shape), the scattered light would at all wave lengths be the same percentage of the total light which is projected optically on to the receptor. No errors due to the scattered light would then accrue.

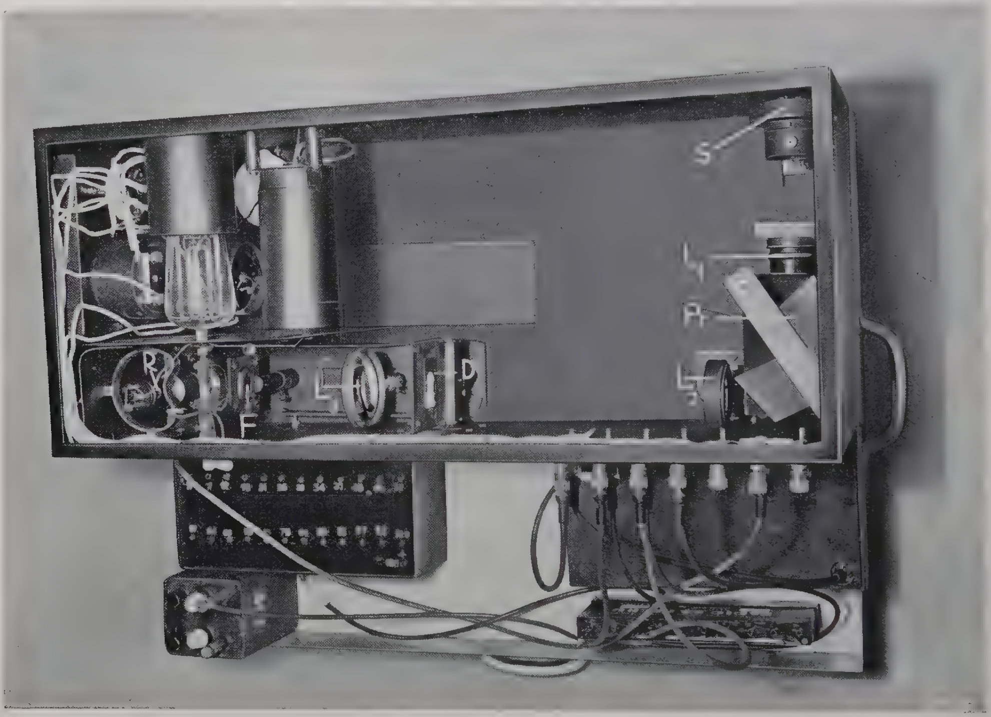

Fig. 3. View of the physical photometer from above, with lid removed. The letters S, L_1, Pr, L_2, D, L_3, F, R have the same signification as in fig. 1.

If the diaphragm is not rectangular, it is principally necessary to compensate for the effect of scattered light, by lowering the screening curve *c* throughout by the same amount. But this can only be done if it does not lead to negative values for the height of the diaphragm. That this case would be likely to occur, may be seen from fig. 2 when considering the blue part of the spectrum:

Since the eye is very insensitive to blue wave lengths, while the photo-cell exhibits a high sensitivity in this range, the scattered blue light alone might already contribute more to the photocurrent, than is wanted from the blue, which contribution can then naturally not be compensated by lowering the height of the diaphragm in the blue.

König ²) suggested in 1934 that spectral adaptation be combined with rough accommodation by means of filters, which would reduce the variations within the screening curve. This would give a more rectangular cut-off of the spectrum. The slit can then be made wider, so that with a given spectral accommodation a greater sensitivity is obtained, and at the same time the difficulties due to scattered light are largely diminished.

This principle used by König also has been adopted for the physical photometer which has been constructed in this Laboratory. The general layout of the instrument has already been given in fig. 1; to the details previously stated, it should be added that a combination of filter *F*, which roughly accommodates the spectral sensitivity curve of the cell to the international luminosity curve, is placed directly in front of the photo-electric cell. The lens L_3 is placed in such a position that the image of the collimator lens L_1 and not the spectrum is projected on to the receptor, a substitution which prevents a variation in the distribution of light over the surface of the cell with an alteration in the shape of the diaphragm superimposed on the spectrum. This precaution is desirable as the spectral

---

²) H. König, Helvetica Physica Acta **7**, 433, 1934.

sensitivity of a photo-sensitive layer is frequently subject to local variations, so that a change in the light distribution might also lead to an alteration in the spectral sensitivity curve. The general appearance of the measuring arrangement may be gathered from *fig. 3* and *4*.

The various parts of the apparatus will now be described separately.

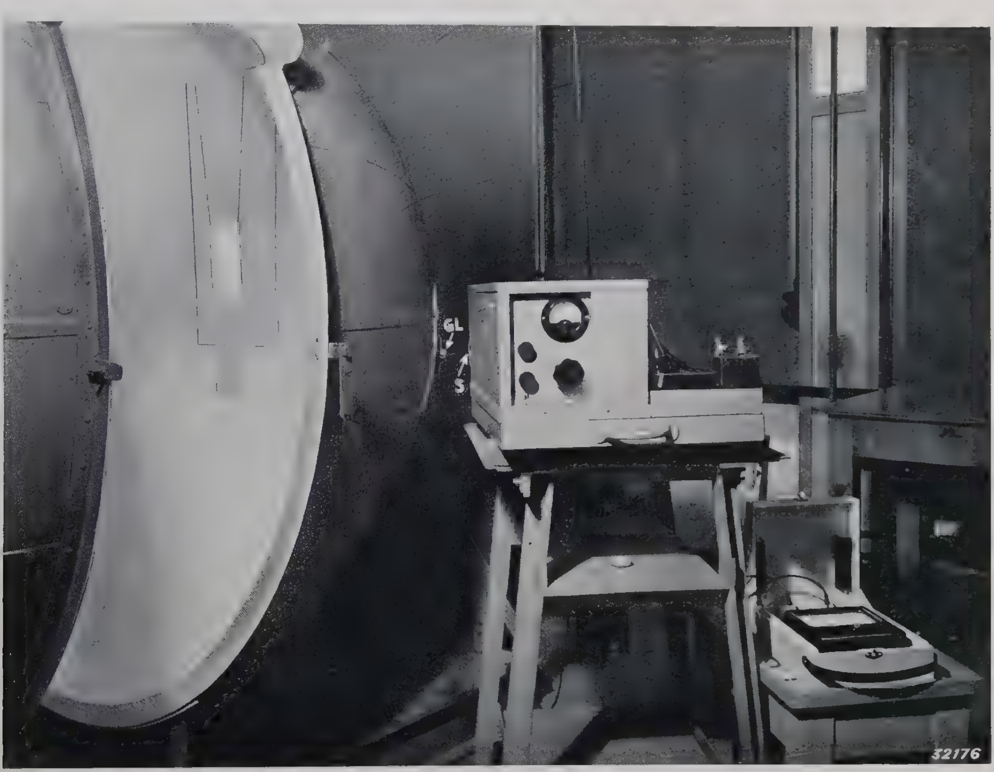

Fig. 4. Rear view of the physical photometer in an arrangement for measuring light fluxes with the aid of an integrating sphere.

Photo-cell, combination of filters and electrical method of measurement

The choice of the receptor has been regarded by us as the most important feature in the design of the apparatus. This receptor must satisfy the following requirements:

1. It should permit a measurement of very small photo-currents; and
2. The relative spectral sensitivity curve should remain sufficiently constant over long periods of time.

The vacuum cell with potassium cathode, Philips 3 510 type, satisfies both requirements and this cell has, therefore, been used by us as a receptor. The spectral sensitivity of these cells varies slightly in different specimens and may exhibit a more or less pronounced maximum. To facilitate accommodation to the international luminosity curve, we selected a cell which did not have an appreciable maximum. The variation of spectral sensitivity is shown in the curves in fig. 2 already discussed and compared with the international luminosity curve. As may be seen from curve *c* in fig. 2 the sensitivity must be reduced not only in the blue and blue-green but also in the red. For a rough correction of the sensitivity curve a combination of the following filters has been used:

Corning Signal Yellow	2.5	mm thick
Corning Noviol A	1.0	mm thick
Schott B G 18	0.75	mm thick

This combination of filters was fixed directly in front of the window of the photo-cell, which is depolished in order to make the distribution of light over the surface of the cell as uniform as possible and hence more constant still than would be achieved by projecting an image of the collimator on the cell window. A good approximation to the international luminosity curve is obtained by the spectral sensitivity of the photocell when combined with the filters, such that the correction of the sensitivity curve by placing a diaphragm in the spectrum needs not be very great, and hence the scattered light does not cause any serious error.

The photo-electric currents must be measured by a very sensitive method, as in measurements with an integrating sphere only photo-currents of the order of 10^{-6} lumens pass through the collimator lens. The application of an electrometric method suggests itself here; an electrometer triode was used as a static voltmeter and the current was measured by electrostatic compensation of the charge liberated by the photo-electric effect from the cathode and which charges the anode of the cell and the grid of the electrometer triode connected to this anode. This method has already been fully described in this Review [3]), so that a detailed description can be dispensed with here.

Production of spectrum

The spectrum required can be obtained in two different ways, either with a reflecting grating or with a dispersing prism. Compared to the prism, the grating offers the advantage that the deflection of the light ray is proportional to its wave length throughout the whole spectrum. In the prism, however, the dispersion is not uniform, and the important spectral region, for instance, between 6 000 and 7 000 Å occupies only a small part of the spectrum. As will be seen later, uniform dispersion as obtained by the grating is particularly valuable in calibration. In the first design of the apparatus a grating was chosen for this very reason and a satisfactory accommodation to the international luminosity curve was arrived at. Nevertheless, a serious drawback of the grating soon appeared, *viz.*, that the reflexion properties of the grating which was ruled on speculum metal did not remain constant, so that the whole apparatus had to be recalibrated at short intervals. Setting up the grating in an inert atmosphere did not improve matters, and the grating was therefore replaced by a prism, whose transmission characteristics remained practically constant if a suitable kind of glass was selected. A higher sensitivity can, moreover, be realised with the prism, for with it practically the whole of the light which passes through the slit on to the collimator lens is utilised in producing a single spectrum, while with the grating the light is distributed over the directly-reflected image and the different-order spectra.

Determination of the required shape of diaphragm

In order to determine the required shape of diaphragm, the spectral sensitivity curve of the apparatus in the absence of the diaphragm was investigated experimentally. This could be done most easily by illuminating the slit with light of a known continuous distribution of spectral energy. For this purpose we used a tungsten ribbon lamp burning at a known temperature, an image of the ribbon being projected on the entrance slit by a photographic lens placed behind a water filter. From the known temperature of the ribbon and the spectral transmission factors of the filter and the lens, of which the last two were measured separately, the relative radiant energy $E(\lambda)$, which passed through the slit per unit of wave band on to the collimator lens could be calculated as a function of the wave length.

To determine the spectral sensitivity, a slit was placed in the plane of the spectrum, this slit being somewhat wider than the monochromatic image of the entry slit, but having the same shape as this (curved) image. This slit could be shifted in the plane of the spectrum. If now $G(\lambda)$ is the sensitivity of the apparatus for light of wave length λ, the photo-current $i(\lambda)$ obtained when the slit is adjusted to transmit the wave length λ will be given by the expression:

$$i(\lambda) = C \cdot E(\lambda)\, G(\lambda)\, \Delta\lambda\,, \quad \dots \quad (2)$$

where C is determined by the apparatus independent of the wave length and $\Delta\lambda$ is the wave band cut-out from the spectrum by the spectral slit and which varies with the wave length.

It follows from equation (2) that:

$$G(\lambda) = \frac{1}{C}\,\frac{i(\lambda)}{E(\lambda)\,\Delta\lambda} \quad \dots \quad (3)$$

To determine from the above equation the sensitivity $G(\lambda)$ as a function of the wave length, the photo-current $i(\lambda)$ must be measured, while the wave length $\lambda(s)$, the corresponding intensity $E(\lambda)$ of the ribbon lamp and the transmitted wave band $\Delta\lambda$ must be known for every position of the slit, which will be defined by an abscissa s. The determination of each of these magnitudes is described below.

The determination of λ and $\Delta\lambda$ as a function of s

If λ is accurately determined as a function of s, the transmitted wave band $\Delta\lambda$ may be calculated. If b is the width of the slit, then to a reasonable approximation we have

$$\Delta\lambda = b\,\frac{\mathrm{d}\lambda}{\mathrm{d}s} \quad \dots \quad (4)$$

λ must be determined very accurately as a function of s, since in certain wave bands the ocular sensitivity varies considerably with the wave length, *e.g.* from 6 000 Å to 6 010 Å by 2 per cent. To measure within 1 per cent, the error in wavelength measurement must be less than 5 Å. For this the abscissal values s must also be measured very accurately, especially as the dispersion in the red is comparatively small. An accuracy to within 5 Å in the red corresponds to an accuracy of about 0.01 mm in measurement of s. The determination of $d\lambda/ds$ from the function connecting λ and s by differentiating makes the need for a high accuracy still greater: $d\lambda/ds$ has been found by measuring the distance apart of spectral lines situated very close together. The spectra of neon, helium and mercury contain a sufficient number of line pairs suitable for this purpose, the difference in wave length being known for these pairs with sufficient accuracy. To be able to measure the distance of these lines with an accuracy of 1 per cent, the position of each line must be determinable to within 2 microns. The requisite degree of accuracy could be obtained by using a comparator.

---

[3]) Philips techn. Rev. 4, 71, 1939.

After having determined λ and $d\lambda/ds$ in this way, the wave band $\Delta\lambda$ in the spectrum transmitted by the slit could be calculated in a relative measure with the aid of equation (4). The width of the slit was varied for measurements in different parts of the spectrum, such that $\Delta\lambda$ was never greater than 40 Å.

Determination of $E(\lambda)$

The colour temperature of the ribbon lamp was 2 725 deg. abs. with an accuracy of ± 25 deg. The effect of this potential error on the distribution of spectral energy $E(\lambda)$ may be gathered from the accompanying table, which gives for a black-body radiator at 2 700 deg. abs. and 2 750 deg. abs. the relative spectral energy flux per unit of time and per unit of wave band for various wave lengths, the flux at 5 600 Å being put equal to 100 at both temperatures. It is seen that only in the extreme red and in the blue an error of 25 deg. in the colour temperature will cause a deviation of more than 1 per cent in the relative distribution of spectral energy. In these parts of the spectrum, the ocular sensitivity is, however, so small that the resulting uncertainty has no practical significance whatever.

Wave length Å	Energy flux at a temperature of	
	2 700 deg. abs.	2 750 deg. abs.
7 000	218.5	211
6 500	176.5	172.5
6 000	133.3	131.8
5 500	92.0	92.5
5 000	56.5	57.6
4 500	29.3	30.6
4 000	12.1	12.9

Measurement of $i(\lambda)$

The photo-current $i(\lambda)$ is the photo-current produced by radiation in the wave band $\Delta\lambda$. As already indicated part of this radiation is scattered, and in calibration this part will not pass through the slit in the spectrum and hence makes no contribution to the value of $i(\lambda)$. It is, however, equal to a constant percentage of the radiation which does pass through, so that its absence alters $i(\lambda)$ only by a factor not depending on λ. As in arriving at the design of the diaphragm, $G(\lambda)$ needs only be known relatively, a correction for this reduction can be dispensed with.

Yet, in calibration, scattered light of other wave lengths also appears, and a portion of this scattered light passes through the slit, giving rise to part of the measured photo-current, so that some correction must be made for it. Take for instance the case when the slit is located in the blue, where the ribbon lamp used for calibration has only a weak radiation intensity. It is evident that then the scattering of the strong red and yellow radiation passing through the slit will produce a serious error, which must be ascertained. This may be done by measuring the photo-currents produced by the scattered red and yellow light separately, using a filter which transmits red and yellow but not blue.

After careful measurement of these corrections for scattered light, the measured photo-currents were corrected. The corrected values of $i(\lambda)$ were used in conjunction with $E(\lambda)$ and $\Delta\lambda$ for calculating $G(\lambda)$.

Having determined the sensitivity, a diaphragm was designed with an aperture at every point of the spectrum which was proportional to $V(\lambda)/G(\lambda)$. This diaphragm is shown in *fig. 5*.

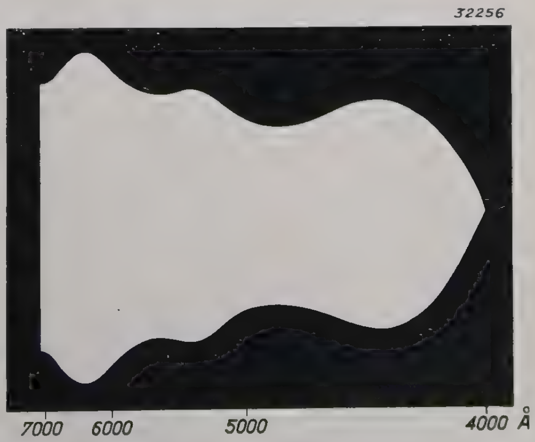

Fig. 5. Shape of diaphragm D used in the physical photometer.

The diaphragm was filed out of a brass plate; to do this accurately a tenfold magnification of the plate was projected on to a sheet of paper on which the diagram was carefully drawn also in a tenfold enlargement. The required shape of diaphragm could then be produced by means of a small file. Using an index for the green mercury line, the diaphragm was then adjusted to the correct point in the spectrum.

Testing the photometer

The photometer can be tested by measuring the intensity ratios of monochromatic light sources with a thermopile and comparing the ratios of luminous intensities calculated from these observations with the results obtained from the photometer. The monochromatic light was produced with the aid of a double monochromator, which in conjunction with a tungsten ribbon lamp furnishes monochromatic radiation of sufficient intensity at wave lengths above 6 000 Å to enable measurements with the thermopile to be carried out. Measurements with the photometer can be made without the diaphragm over the spectrum. The maximum differences in comparative measurements at five different wave lengths did not exceed 3 per cent.

To enable measurements to be made also in the yellow and green, the yellow and green mercury lines were filtered out with suitable filters and again measured by both the photometer and the thermopile. At these wave lengths the calibration of the photometer was found to be accurate to within 1 per cent.

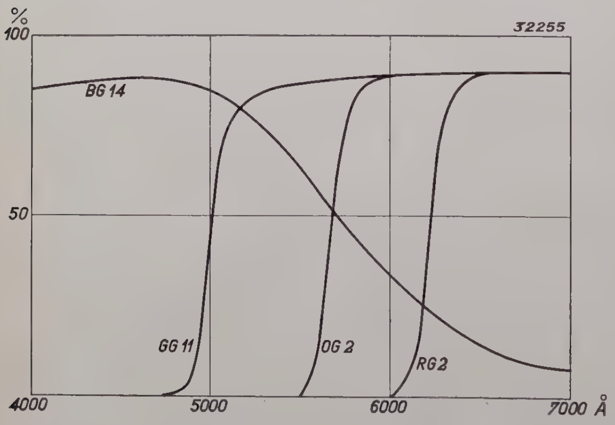

Fig. 6. Spectral transmission curves of the filters used for check measurements.

Finally, to afford a further test of the accommodation to the international luminosity curve, the total transmissibility of several filters for the light of a ribbon lamp, burning at a known colour temperature, was measured with the photometer. In addition, with a double monochromator and a photo-cell the spectral transmission curves of these filters were determined and the theoretical values of the total transmission were calculated from these transmission curves in conjunction with the colour temperature and the international luminosity curve.

The results are given in the following table, which shows that agreement between the measured and the calculated transmission values is very close. *Fig. 6* reproduces the spectral transmission curves of these filters, indicating that this test ensures that correct accommodation has been realised.

Filter	Transmissibility	
	Calc.	Measured
Schott BG 14	49.4	49.2
Schott RG 2	11.8	11.9
Schott OG 2	49.5	50.0
Schott GG 11	85.7	86.3

Sensitivity

In visual photometry, it is essential to have a minimum brightness over the field of vision of 8 candles per sq. m. To measure the photo-current with the apparatus described here with an accuracy of 1 per cent, the brightness of the illuminated surface placed in front of the slit must be 130 candles per sq. m. The physical photometer described is, therefore, 16 times less sensitive than the eye, a comparison applying for a slit width of 0.3 mm and a collimator lens with an aperture f/6.8. Although the sensitivity is sufficient for practical purposes, it can quite easily be improved eight times by making the slit wider and by using a more powerful collimator lens. The apparatus in question hence satisfies the requirements which must be met by a precision physical photometer, both in affording accurate accommodation of its spectral sensitivity curve and in affording a sensitivity comparable to that obtained in visual photometry.

AN ELECTRON SWITCH

by C. DORSMAN and S. L. de BRUIN.

621.317.755.06

An apparatus is described with which the time function of two different magnitudes can be observed simultaneously on the fluorescent screen of a cathode-ray oscillograph. A number of practical examples are discussed where such investigation is of value, *inter alia*, the simultaneous registration of vibrations at different points of a mechanical system or of the current and voltage conditions in a transformer.

With the aid of a cathode-ray oscillograph, such as the GM 3152 recently described in this Review [1]) the image of an electrical tension can be represented on the fluorescent screen of a cathode-ray tube in relation to a second voltage. If a linear time base is used, the curve of the variation of the voltage with time can then be projected on the screen. In addition, a third variable is available, *viz.*, the intensity of the cathode beam which can be modulated in relation to a third magnitude. In this way two magnitudes can be simultaneously represented as a function of the time, displacements in phase in the magnitudes under measurement being revealed in the projected images. But this method does not reveal any small variations in the third magnitude, so that it becomes essential to devise an apparatus for registering two curves simultaneously showing the variation with time of two different voltages. Apparatus designed for this purpose have often been described in the literature, and their underlying principle has also been discussed in this Review [2]). The present article gives a description of an apparatus, the socalled electron switch GM 4196, which has been devised for this purpose, together with details of certain of its applications. A view of the measuring outfit, consisting of the electron switch and its associated cathode-ray oscillograph GM 3152, is shown in *fig. 1*.

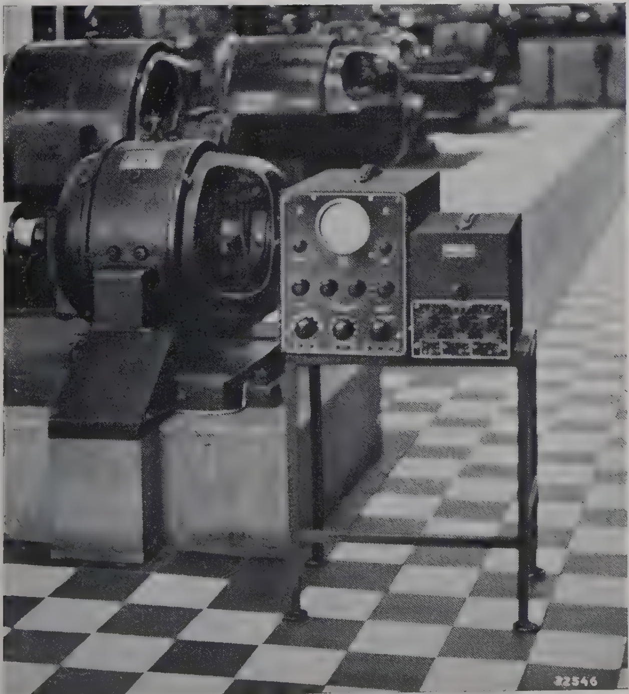

Fig. 1. Measuring arrangement comprising an electron switch, Type GM 4196, and the associated cathode-ray oscillograph, Type GM 3152.

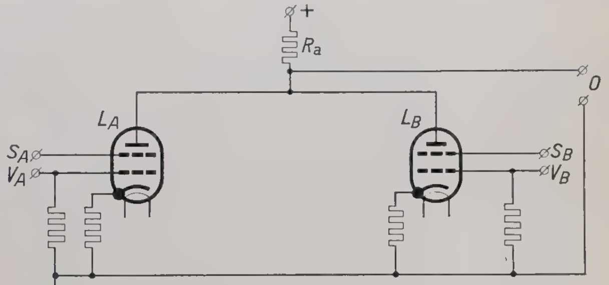

Fig. 2. The two voltages V_A and V_B to be observed simultaneously by the cathode-ray oscillograph O are applied to the control grids of the pentodes L_A and L_B. The switching voltages S_A and S_B varying rectangularly with time are applied to the screen grids. The anodes of L_A and L_B are connected through a common anode resistance R_a to a constant positive voltage.

Method of operation of the electron switch

A circuit is shown in *fig. 2* with which the time functions of two electrical tensions V_A and V_B can be represented simultaneously. These two voltages are impressed on the control grids of the two pentodes L_A and L_B, and an alternating voltage of 10 000 cycles frequency varying rectangularly with time is applied between the two screen grids. This voltage is of such a magnitude that the two valves L_A and L_B alternately either function in the normal way or are in such a state that no anode current passes through the valve. In consequence of this, a current passes through the common anode resistance R_a which flows alternatively through L_A and L_B and is hence controlled in turn by the tensions V_A and V_B at the control grids of L_A and L_B. The voltage through R_a thus fluctuates with a frequency of 10 000 c/s between two values which are determined by V_A and V_B respectively. If, now, the anode voltage is applied to the first pair of deflecting plates of the cathode-ray oscillograph O, while a linear time base is applied to the other pair of plates, an image of the type shown in *fig. 3* will be projected on the screen.

---

[1]) Philips techn. Rev. **4**, 210, 1939.

[2]) *Cf.* also Philips techn. Rev., **3**, 154, 1938.

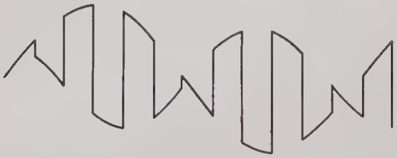

Fig. 3. Oscillograph image obtained when two oscillograms are registered simultaneously with the aid of the electron switch. Actually the number of impulses is, of course, much greater than sketched here.

To ensure that the light spot travels sufficiently swiftly between the projected curves (fig. 3) of V_A and V_B, the amplifier must be suitable for amplifying a rectangular oscillation of 10 000 cycles per sec. It must, therefore, be able to amplify not only the fundamental wave of 10 000 cycles but also have roughly the same gain for a large number of harmonics of this fundamental wave. In the cathode oscillograph GM 3152 the gain remains practically constant up to 10^6 cycles, so that the hundredth harmonic is not yet severely attenuated.

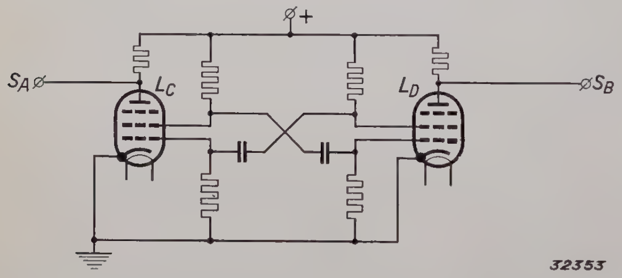

Fig. 4. Circuit for generating the switching voltages S_A and S_B varying rectangularly with time, at the anodes of the pentodes L_C and L_D, whose control and screen grids are capacitively coupled with each other.

Fig. 4 shows the circuit used for obtaining the alternating voltage varying rectangularly with time and which is required for the screen grids of L_A and L_B. In principle this circuit represents a multivibrator as designed by Abraham and Bloch. Between the two corresponding pentodes L_C and L_D two condensers are connected which link the control grid of each of these valves with the screen grid of the other valve of the pair. The state of equilibrium, which would be obtained if the voltages of the control grids for the two valves were equal, and likewise those of the screen grids for the two valves, is found not to be stable. If, for instance, at a certain moment the voltage at the control grid of L_C is too high the current through L_C will increase, so that a greater amount of current will have to be dissipated by the screen grid resistance of L_C, which will reduce the screen grid voltage of L_C and owing to the capacity coupling also cut down the control grid voltage of L_D. A lower current will then flow through L_D and the screen grid current of L_D will fall, and hence the voltage at the screen grid of L_D will rise. The presence of the capacity coupling will then also raise the voltage at the screen grid of L_C. The condition of the circuit hence will be labile, since we started with the assumption that the control grid voltage at L_C was already too high. The increase in the voltage at the screen grid of L_D is limited by the anode voltage to which the screen grid is connected over a resistance. If the screen grid voltage of L_D cannot increase further, the control grid of L_C will discharge itself through its resistance leak, with the result that the whole process will be repeated in the opposite direction. The relaxation time of this oscillation is hence determined by the capacity and the leak resistance of the control grid.

If now the anode voltages of L_C and L_D, which vary roughly rectangularly with the time, are applied to the screen grids of L_A and L_B, these valves will be working or idle in turn, so that the amplified voltage V_A and V_B are applied alternately to the deflecting plates of the cathode-ray tube. Since the oscillator circuit lies between the screen grids of of L_C and L_D, while the reversing voltages are taken from the anodes of these valves, the oscillator is practically unaffected by the voltages which may be applied to the valves L_A and L_B and which are to be registered by the oscillograph.

Assume that the voltages V_A and V_B to be registered have constant values and are equal to one another and that changing-over takes place instantaneously by means of pure rectangular anode voltages of L_C and L_D, the total anode voltage of

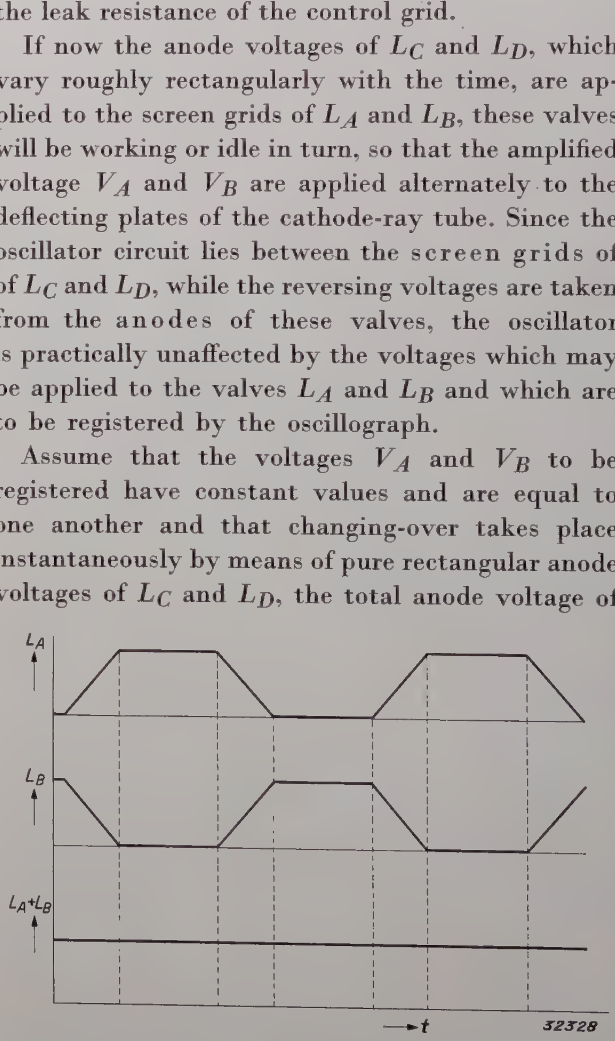

Fig. 5. Anode currents of the pentodes L_A and L_B if they are increased and decreased linearly with time.

L_A and L_B will then also be constant and there will be no indication on the screen of the changing-over operation. This would still be the case if the anode currents of L_A and L_B during changing-over varied linearly with the time as shown in *fig. 5.*

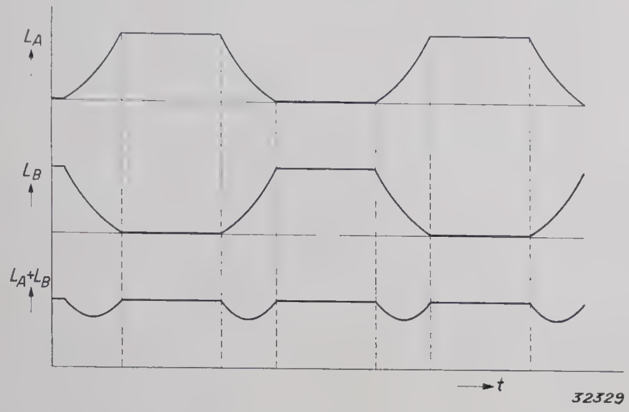

Fig. 6. Actual shape of the time functions of the anode currents of L_A and L_B and of $L_A + L_B$.

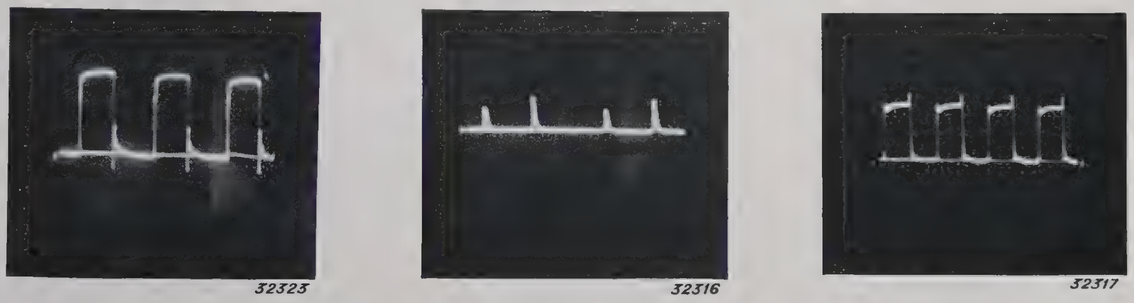

a b c

Fig. 7. The shape of the switching voltages S_A and S_B is shown in fig. *a*). The shape of the socillogram for $V_A = V_B$ is shown in fig. *b*), and for $V_A \neq V_B$ in fig. *c*).

Actually, however, the flanks of the anode current impulses of L_A and L_B are always curved (*fig. 6*), so that the total anode current which passes through R_a, and hence the tension across R_a, will show small troughs. The voltage between anode and earth, which is passed to the oscillograph, will therefore reveal small peaks at the moments of changing over from one of the voltages to be registered to the other, both when the two voltages are equal and when they differ (*fig. 7*). These unavoidable irregularities can, however, be minimised by making the current impulses as steep as possible, when the peaks are barely visible, as shown in *fig. 8.*

Shape of projected curves

The curves registered simultaneously by the oscillograph when using the electron switch are made up of short dashes which must follow each other in such close succession that fairly sharp and smooth curves become visible on the screen. To obtain this result it is not enough to make the switching signals purely rectangular, so as to obtain a swift change-over from one image to the other, but, in addition, the frequency of reversal per second must be made so great that the large number of small dashes appear to the eye to merge into a smooth and continuous curve. If a switching frequency of 10 000 cycles per sec. is employed, the oscillogram of a function with a periodicity of 50 will show practically no breaks, as may be seen from fig. 8. Furthermore, the tenth harmonic of 50 cycles, whose frequency is 1/20 of the switching frequency, will also still have a satisfactory outline. If a switching frequency lower than 10 000 cycles were used, the subdivision of the oscillation of 500 cycles would become too coarse, while if the periodicity were made very much greater than 10 000 c/s difficulties would arise in obtaining switching signals with a sufficiently rectangular time function, since the capacity of the current-carrying parts gives too low an impedance for these high frequencies.

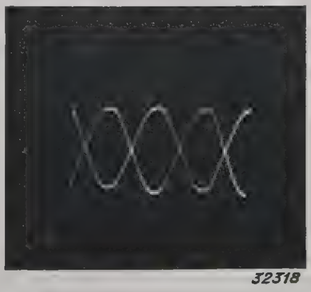

Fig. 8. With the electron switch two curves are obtained which to the eye appear to have a continuous outline.

Registration of mechanical oscillations

To register mechanical oscillations with a cathode-ray oscillograph, these must first be converted into electrical voltages, for which e.g. an electrodynamic system can be employed: an electrical coil moves in the field of a permanent magnet (*fig. 9*), the coil being attached to the object whose vibrations are under investigation.

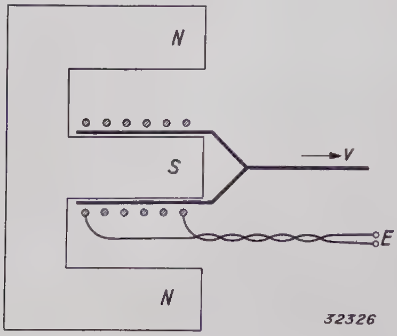

Fig. 9. A coil oscillates in the field of a stationary magnet with north-pole N and south-pole S. In the moving coil electrical tensions E are induced which are proportional to the velocity of deflection v.

In the moving coil an electrical voltage is induced which is proportional to the velocity provided the deflections sustained are not too great. If the oscillations at two different points of a mechanical system are imparted to two different coils, both oscillations can be registered simultaneously by a cathode-ray oscillograph with the aid of the electron switch, thus permitting direct visual comparison with respect to amplitude and phase.

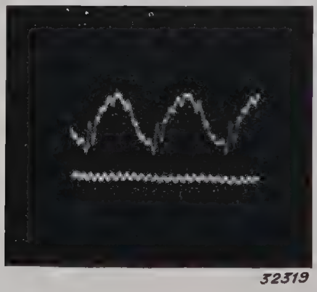

Fig. 10. The large amplitude represents the mechanical vibration of an electric motor, while the small amplitudes reproduce an alternating voltage with a standard frequency of 500 cycles per sec.

The voltage induced by a mechanical vibration can also be registered in conjunction with another magnitude on the screen of the cathode-ray tube; thus in *fig. 10* the vibrations of an electric motor (with a large amplitude) are compared with an alternating voltage of 500 cycles as normal frequency (small amplitude). This comparison shows that the frequency of the fundamental wave of the vibration is 53 cycles, so that the motor is running at a speed of about 3 200 r.p.m. The fundamental wave of the oscillation also contains a number of notches; this oscillation of much higher frequency has been produced by one of the moving parts rubbing at some point or other. The frequency of this disturbance is 530 cycles.

Phase displacements between currents and voltages

It is frequently important in the examination of electrical plant to determine not only the time functions of various currents and voltages but also to know the phase relations of these magnitudes. With the aid of the electron switch, both current and voltage may be projected simultaneously on to the screen of an oscillograph, so that the phase relations are directly visible. In an issue of this Review which appeared last year, the combined oscillograms of currents and voltages of a gas discharge lamp were reproduced and discussed. Another example may be mentioned here, *viz.* the current and voltage conditions in a circuit containing a transformer with an iron core so highly saturated that the secondary voltage remains practically constant when large variations occur in the primary voltage. The principle of operation of a stabiliser of this type (*fig. 11*) has already been described in this Review [4]). If a pure sinusoidal voltage is applied to the primary side, a voltage which is heavily flattened (*fig. 12a*), *i.e.* with a considerable amount of third harmonic, is obtained on the secondary side owing to the high saturation of the iron. The curve of the primary current also indicates a pronounced third harmonic, which,

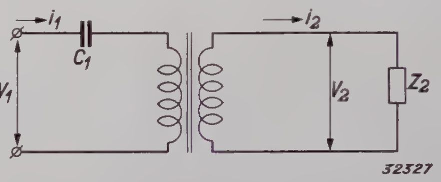

Fig. 11. Circuit of a transformer with a highly-saturated iron core, as a result of which the secondary voltage remains practically constant, although the primary voltage may fluctuate widely. V_1 and V_2 are the primary and secondary voltages respectively, and i_1 and i_2 the primary and secondary currents. Z_2 is the load, which is principally capacitative (an apparatus for anode-volts).

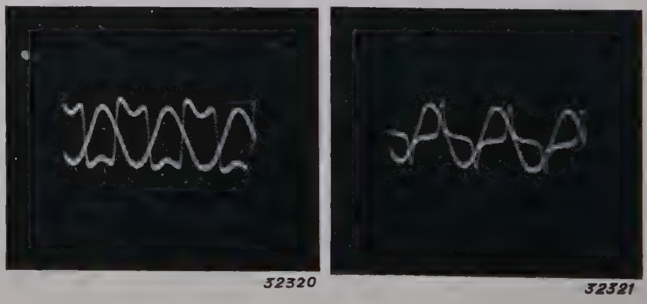

a b

Fig. 12. The sinusoidal curve represents the primary voltage impressed on the transformer; the flattened curve in *a*) is the secondary voltage, and the peaked curve in *b*) the primary current, which both have a pronounced third harmonic.

---

[3]) Philips techn. Rev. **3**, 156, 1938.

[4]) Philips techn. Rev., **2**, 279, 1937.

however, augments the maxima, as may be seen clearly in fig. 12*b*. Furthermore the figure reveals that both primary current and secondary voltage are somewhat delayed with respect to the primary voltage.

Registration of pulsating direct voltages

As ordinary electrical amplifiers only amplify alternating voltages, an oscillograph will usually reveal only the A.C. component of pulsating direct voltage. One of the main advantages of the electron switch is that it enables us to study also the direct-voltage component with the oscillograph, since it converts the direct voltage into an alternating voltage of the switching frequency used, and for which the amplifier of the oscillator happens to be particularly suitable.

In the oscillograms in *fig. 13* the two curves show the zero line of the voltage and the pulsating direct voltage of a source of anode voltage. With a low load of 100 milliamps the ripple of this direct voltage is obviously only small (fig. 13*a*), while a pronounced pulsation is shown with a heavy load of 500 milliamps (fig. 13*b*).

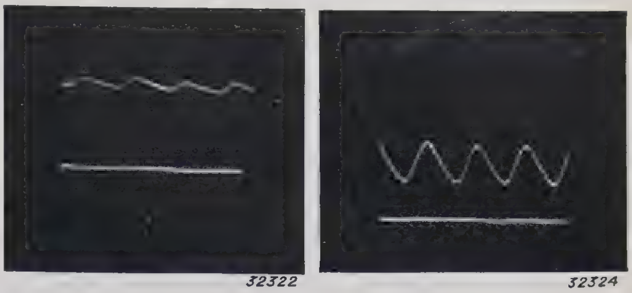

a b

Fig. 13. The oscillogram of a pulsating direct voltage as well as the zero line can be registered with the electron switch.
a) The voltage of an anode-volts supply reveals a small ripple at a load of 100 milliamps.
b) At a load of 500 milliamps the curve shown in *a*) acquires a heavy pulsation.

AN ELECTRICAL MEGAPHONE

by J. de BOER.

621.395.61

A portable electrical voice amplifier, the "Portaphone" Type No. 2 831, has been devised to obtain a greater range of the human voice than when speaking normally without directive aids or when using an ordinary megaphone. This apparatus increases the intensity of the sound energy 30 to 100 times the gain realised with an ordinary megaphone. Hence, the range of the voice is 5 to 10 times larger with the "Portaphone" than with an ordinary megaphone.

In ordinary speech the range of the human voice is not very great, and various means have therefore been devised for increasing the range to which the voice will carry. The oldest of these aids is the speaking tube or megaphone which was invented about the middle of the seventeenth century by the German divine Kircher and the Englishman Morland. Its action consists in imparting a directivity to the sound waves so that they are concentrated into a narrow beam with a small solid angle. Recent developments in amplifying technology have, however, raised the question whether better results in the transmission of the human voice over great distances could not be realised with the aid of a simple electrical amplifier. While retaining the concentrating effect of the megaphone horn, an apparatus of this type would moreover provide a source of sound which is more powerful than the human voice.

In constructing such a simple voice amplifier, the first requirement is to arrive at maximum convenience in use. The loudspeaker, horn, and microphone should form a compact unit which can be conveniently carried in the hand, while the electrical amplifier may be accommodated in a separate case. The „Portaphone", Type No. 2 831, which has been designed on these general lines, is shown in *fig. 1*; the carbon microphone is mounted in the loudspeaker which also carries a horn and a handle with switch. The flat case containing the electrical amplifier is carried by a strap; its total weight is 6.8 kg. and in addition to the amplifier also holds a 2-volt accumulator to furnish the filament current and to feed the microphone, as well as dry batteries for the grid and anode voltages up to 150 volts. The electrical gain is approximately 40 decibels. The acoustical gain is somewhat lower owing to losses in microphone and loudspeaker (*cf.* at the end of this article). The amplifier furnishes an output of 3 watts with a non-linear distortion factor of 5 per cent, and an output of 4 watts with a non-linear distortion factor of 12.5 per cent. The accumulator requires recharging after every five-hours use.

An important factor in the construction of a simple voice amplifier of this type is the method of fixing the microphone on the loudspeaker; for, if suitable precautions are not taken, the mechanical or acoustic coupling between these components may be made too rigid. A mechanical coupling may result by the loudspeaker frame imparting vibrations to the microphone, and an acoustic coupling by the sound waves on leaving the horn being deflected to such a degree that part of them again strike the microphone. The two couplings must be sufficiently reduced, so that the whole system, with a given sensitivity, remains stable.

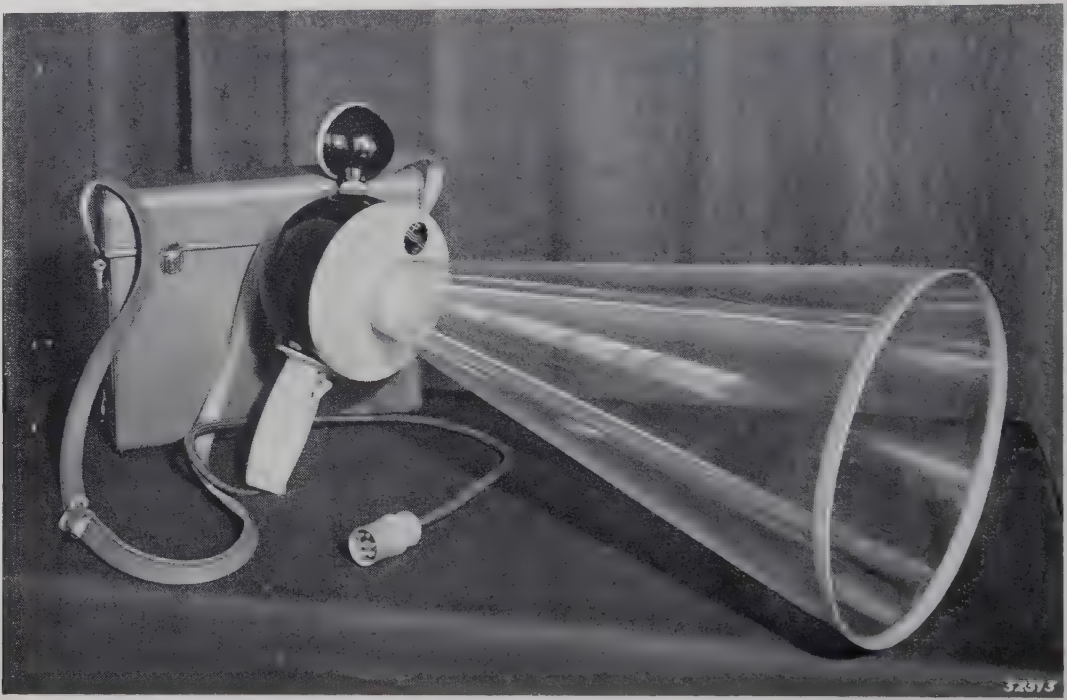

Fig. 1. The "Portaphone", Type No. 2831, consisting of a microphone attached to a horn loudspeaker mounted on a handle, and an electrical amplifier in a flat case carried by a strap.

To reduce the mechanical coupling the microphone is given a spring suspension, whose action may be discussed with reference to *fig. 2* in which the principle of the arrangement is shown. The amplitudes y produced in the microphone with mass M should be small as compared with the deflections x of the frame C to which the microphone is attached by a spring with a rigidity S. If the frame is subject to harmonic oscillation with a frequency $\omega/2\pi$, x may be represented by the expression:

$$x = a \sin \omega t. \quad . \quad . \quad . \quad . \quad . \qquad (1)$$

Neglecting damping the deflection of the microphone will then be:

$$y = \frac{a \sin \omega t}{1-\left(\frac{\omega^2}{\omega_0{}^2}\right)}, \quad . \quad . \quad . \quad . \quad . \qquad (2)$$

where $\omega_0/2\pi$ is the resonance frequency for a mass M attached to a spring with rigidity S. If a sufficiently slack spring is used to make this resonance frequency much lower than the lowest frequency at which it is sought to avoid mechanical coupling ($\omega_0 \ll \omega$), the amplitude y of the microphone will be much smaller than that of the frame. In fact at very high frequencies the amplitude y will diminish with the square of the frequency: $y \sim -(\omega_0/\omega)^2 x$.

The acoustic coupling can be limited in magnitude by making the horn not too short, so that the mouth of the horn and the microphone are placed far enough apart; on the other hand if the horn is made too large the apparatus becomes too clumsy to handle and acoustic coupling must then be avoided by other means. A very important factor here is the point at which the microphone must be attached to the loudspeaker. The sound pressure is the same in all spacial directions behind the loudspeaker when the wave length is large compared to the dimensions of the loudspeaker, *i.e.* for sufficiently low-pitched notes; thus, for these notes it is immaterial where the microphone is attached to the loudspeaker. For high-pitched notes, however, the sound pressure behind the loudspeaker is by no means constant, and the microphone preferably must be fixed in a point, where the sound pressure is a minimum. Except for simple geometrical bodies, such as a sphere or a cylinder, a calculation of the pressure at the rear of the speaker is usually not practicable. It may only be stated that in the case of a solid of rotation the sound pressure is a maximum along the rear axis. On a model of our loudspeaker, the distribution of sound pressure was therefore measured at different frequencies, the results being shown in *fig. 3* with frequencies of 1 000 (*A*) and 2 000 cycles per sec (*B*). The best position for the microphone is roughly at an angle of 45 deg. to the rear and is marked with a circle.

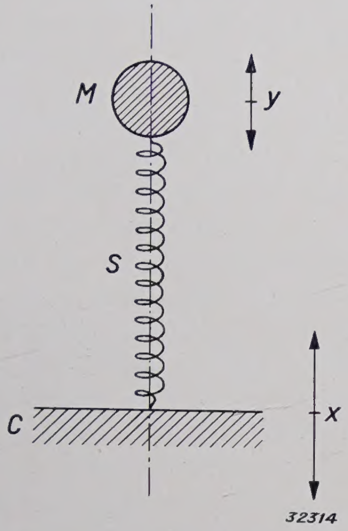

Fig. 2. Sketch of the spring suspension of the microphone of mass M at a spring with a rigidity S, which is attached to the frame C. A displacement x of the frame causes a displacement y of the microphone, which must be much smaller than x.

To limit the acoustic coupling at low frequencies, the sensitivity of the amplifier must be reduced for these frequencies, which can be done without affecting the intelligibility (*cf.* R. Vermeulen, Philips techn. Rev. 3, 140, 1938). This cutting-off of the low-pitched notes may be done in either the amplifier, the loudspeaker (by introducing a high resonance frequency), or the horn: according to the dimensions of the latter, notes below a certain frequency will be radiated with a lower intensity. In our design we used a conical horn with an angle at the apex of approximately 20 deg., the limiting frequency being in the region of 300 cycles. The electrical amplifier and the loudspeaker, also, are less responsive to tones below 300 cycles than to higher tones.

The electrical megaphone, shown in fig. 1, amplifies the human voice by 25 or 30 decibels, according as the electrical gain is partly or wholly utilised. This efficiency is quite satisfactory, if it is remembered that an ordinary megaphone gives a gain of only 10 decibels corresponding to an increase of the range of the human voice by about three times. With the "Portaphone", however, this range is increased 15 to 30 times. If there is little extraneous noise in the vicinity, the voice can thus be heard intelligibly to a distance of over 300 m when speaking normally.

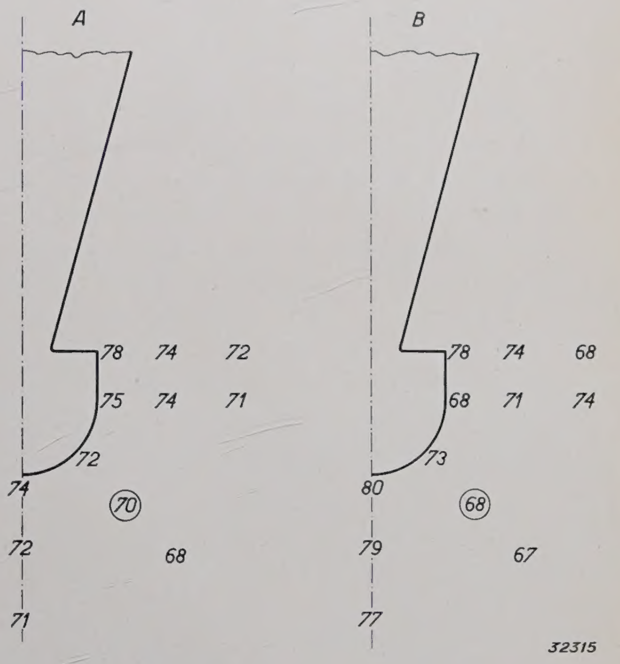

Fig. 3. Measurements of the sound pressure in the neighbourhood of the "Portaphone", this pressure being expressed in decibels above an arbitrary base level, *A* at 1 000 and *B* at 200 cycles per sec. The best position for the microphone is marked by a small circle.

ABSTRACTS OF RECENT SCIENTIFIC PUBLICATIONS OF THE N.V. PHILIPS' GLOEILAMPENFABRIEKEN

1396*: F. A. Heyn: The reaction between neutrons and matter (1). (in the Dutch periodical: Ned. T. Natuurk. **6**, 25-50, Feb. 1939).

This article gives a survey of the different reactions which may take place between neutrons and atomic nuclei.

1397: W. Uyterhoeven et C. Verburg: Température des électrons T_e dans une décharge en colonne positive à courant alternatif (50 périodes par seconde). Résultats pour le néon. (C. R. Acad. Sci. Paris **208**, 269-271, Jan. 1939).

According to the method described in **1380** at each phase of the 50 period alternating current the electron temperature is measured in neon in a positive column discharge. The current-voltage characteristics of the probe electrodes have the same form as for direct current. The variation of the electron temperature with time is found analogous to the variation of voltage at the terminals of the lamp. The electron temperature with an alternating current discharge at a pressure of 70 mm is not constant over the whole cross section, but is higher along the axis than at the circumference, while with a direct current discharge the electron temperature does not depend upon the distance from the axis. In order to obtain the necessary homogeneity and stability of discharge for the measurement, low tension arcs were introduced at the electrodes as auxiliary discharges.

1398*: W. G. Burgers: Metallographic investigation with the electron microscope (in the Dutch periodical: Polytechn. Wkbl. **33**, 17-18, Jan. 1939, and 38-40, Feb. 1939).

This is a survey of the material contained in earlier publications of the same author, for which we may refer to: Philips techn. Rev. **1**, 312, 321, 1936.

1399: J. L. Snoek: Magnetic aftereffect and chemical constitution (Physica **6**, 161-170, Feb. 1939).

By means of a series of heat treatments in an atmosphere of a precisely determined composition it is proved that the ferromagnetic retardation phenomena described in **1339** (dependence on time, not only of the induction but also of the permeability) were caused by the presence of a small amount of carbon (about 0.008 %) in the otherwise very pure iron. Entirely analogous phenomena occur when equal quantities of nitrogen are added to the same iron. The constant r_1 from the formal theory of **1339** is found to be proportional to the concentration of nitrogen (carbon). A tentative theory of the specific action of these two elements is proposed, which is based on the great mobility of these atoms. It is assumed that the atoms of nitrogen (carbon), under the influence of magnetostrictive forces, diffuse out of or into the boundary layers between the elementary ferromagnetic regions.

1400*: M. J. Druyvesteyn und J. G. W. Mulder: Fortschritte auf dem Gebiete der Lebensdauer von Gleichrichterröhren mit Oxydkathode und Gasfüllung (in the Czech periodical: Slaboproudy Obzor **4**, 1-4, Jan. 1939).

A survey is given of experiments on cathode sputtering and the disappearance of gas during discharge with different forms of hot cathode and different kinds of gas filling. It is found that at pressures of less than 1 mm, discharge tubes filled with krypton and xenon have a surprisingly long life and are particularly adapted for use as rectifier valves.

1401: W. Uyterhoeven et C. Verburg: Température des électrons T_e dans une décharge en colonne positive à courant alternatif (50 périodes par seconde). Mesures dans un mélange Ne-Na (lampes à vapeur de sodium). (C. R. Acad. Sci. Paris, **208**, 503-505, Feb. 1939).

According to the method described in **1380** the electron temperature is measured at each phase of the alternating current of 50 periods in a mixture of sodium and neon such as exists in sodium lamps. The terminal voltage and the electron temperature at different distances from the axis are given as a function of the phase. At the beginning of a phase the sodium atoms are still distributed uniformly over the whole cross section of the tube, so that the electron temperature then has practically the same low value throughout the entire tube. As the current increases the available sodium atoms disappear due to ionization; the electron temperature thus rises, beginning at the axis of the discharge, since the current density is greatest at that place. When the current is at a maximum, the electron temperature is much higher along the axis of the tube than at its circumference.

---

*) An adequate number of reprints for the purpose of distribution is not available of those publications marked with an asterisk. Reprints of other publications may be obtained on application to the Natuurkundig Laboratorium, N.V. Philips' Gloeilampenfabrieken, Eindhoven (Holland), Kastanjelaan.

1402: J. D. Fast: The preparation of pure titanium oxides (Rec. Trav. chim. Pays Bas **58**, 174-180, Feb. 1939).

A method is described for the preparation of the pure tetra, tri and diiodides of titanium. Upon heating the triiodide above 350°C in a high vacuum it decomposes into di and tetraiodide. If the diiodide is heated in a high vacuum above 480°C it decomposes partially into titanium and the tetraioddide of titanium, while at the same time part of it evaporates without decomposing. The gas phase in equilibrium with solid titanium iodide therefore consists of a mixture of tetra and diiodide. Several other properties of the iodides are discussed.

1403: C. J. Bakker and G. Heller: On the Brownian motion in electric resistances (Physica **6**, 262-274, Mar. 1939).

It is shown in this article how it is possible to derive from very general statistical considerations that the variation in the mean square of the voltage V on a resistance R in a frequency region $\Delta \nu$ at the absolute temperature T can be represented by the well known expression: $\Delta V^2 = 4\,k\,TR\,\Delta \nu$. The influence of the chance of collision of the electrons is further dealt with making use of Fermi and Boltzmann statistics.

1404: W. Elenbaas: Ueber das kontinuierliche Spektrum des Quecksilberbogens (Physica **6**, 299-302, Mar. 1939).

The expression derived by Unsöld for the intensity of the continuous spectrum of the highpressure mercury arc is tested carefully by measurements. The intensity measured is found to be about ten times as great as that calculated. Due to the inaccuracy of various quantities used in the calculation, an inaccuracy of this order of magnitude can, however, be fully explained, so that it is still possible that Unsöld's formula is quite correct.

1405*: M. J. O. Strutt: Etages à haute fréquence, étages changeur de fréquence et détecteur des récepteurs de télévision (Onde él. **18**, 14-26 and 83-91, Jan. and Feb. 1939).

It is shown that the input signals in television must be at least 1 or 2 millivolts in order that they may be higher than the noise level. This fact necessitates an amplification of about 5 000 between the aerial and the second detector. A scheme for a receiver used by Philips in 1936 is described and two newly developed schemes are discussed. Direct high-frequency amplification is described in which two new valve types are used in the three stages between aerial and second detector. The construction of an experimental installation is discussed as well as measurements carried out on this installation. The calculations and measurements led to a general study of the conditions which the valves in television receivers must satisfy. A mixing stage is then described and a corresponding superheterodyne television receiver in which the newly developed valves are used. In conclusion the conditions are studied which must be satisfied by a diode used as second detector in a television receiver. A new diode is described which is suitable for this purpose.

A similar article (**1427**) by the same author has since appeared in the Wireless Engineer **16**, 174 - 187, Apr. 1939, reprints of which are available, and to which we may refer for further information.

1406: W. Elenbaas: The temperature in the high pressure mercury discharge tube (Phys. Rev. **55**, 294 - 296, Feb. 1939).

Various arguments are presented which confirm the opinion that the temperature of the gas and of the electrons in a high pressure mercury discharge decreases very gradually from the centre toward the walls, and does not, as indicated by Adams and Barnes, remain constant over a large part of the cross section and decrease very rapidly close to the wall. It is shown moreover that the difference between gas temperature and electron temperature is considerably smaller than Adams and Barnes assume.

1407 - 1408: J. M. Stevels: New aspects on the cohesion of simple compounds (Rec. Trav. chim. Pays Bas **58**, 229 - 243 and 244 - 256, Mar. 1939).

It is shown that the contribution of the partial dipole moments to cohesion can better be described as a Keesom effect in a general sense, as was recently proposed by Staverman. The Debye effect must then be considered as mainly due to the total dipole moment of the molecules. On this basis various difficulties, which were until now encountered in the theory of boiling points, can be solved. A complete survey is given of all the phenomena which influence the boiling point. Theoretically the sum of the contributions of the Debye and Keesom effects to the boiling point of halogen compounds of methane, ethane and ethylene must be about constant. It is shown that this is also true experimentally. A complete list of boiling points is given of the compounds of ethane and ethylene, and those of the methane compounds are given in so far as they have not been published by van Arkel and his collaborators. The boiling points are divided into different parts due to the different kinds of cohesion effects. The so called anomalies in the boiling points of the two 1,2 isomers of $C_2H_2J_2$ and C_2H_2ClJ can now also easily be understood.

1409: J. D. Fast: Über die Darstellung der reinen Metalle der Titangruppe durch thermische Zersetzung ihrer Jodide. V. Titan (Z. anorg. allg. Chem. **241**, 42 - 56, Mar. 1939).

A description is given of the preparation of ductile titanium by thermal decomposition of titanium iodide on a hot wire, and of the preparation of the necessary crude titanium. When porous lumps of titanium with dimensions of several centimetres are used, such as can be obtained by the reduction of titanium tetrachloride with sodium, and with the core wire heated to a suitable temperature (1 300 °C for instance), the metal is not deposited on the core at any desired high temperature of the Pyrex glass reaction vessel. Between 50 and 250 °C and above 470 °C the metal is formed on the wire, but between 250 and 470 °C the core wire does not grow. When the reaction vessel has once been heated above 400 °C the reaction can no longer take place at any temperature under 470 °C. This is due to the reaction occurring above 100 °C between titanium tetraiodide and excess titanium in which one or two lower iodides are formed. In the low temperature range the vapour consists only of TiI_4, but at higher temperatures it also contains TiI_2. Small quantities of oxygen and nitrogen which may be present in considerable amount in solid solution, destroy the ductility of titanium. For various other impurities, such for example as iron, the ductility is not so sensitive. If one begins with crude titanium containing 3.5% of iron, titanium rods can be obtained in the high temperature range which contain so little iron and silicon that they can only be detected spectroscopically.

1410: F. A. Heyn, A. H. W. Aten jr. and C. J. Bakker: Transmutation of uranium and thorium by neutrons (Nature **143**, 516 - 517, Mar. 1939).

With the aid of the extremely strong source of neutrons of the Philips X-ray Laboratory the experiments of Hahn and Straßmann were continued. It was found that with a bombardment by slow neutrons a radioactive gas was formed from uranium. Nitrogen was allowed to bubble through a saturated solution of uranylnitrate which was being irradiated. The nitrogen was then led through a vessel containing water. When salts of caesium, rubidium, barium, strontium and lanthanum are added afterwards to the water, radioactive substances are found to be precipitated together with caesium, rubidium and barium. The half lives of these substances were determined. The results led to the conclusion that the nucleus of the uranium atom can disintegrate in at least two different ways with the formation of xenon and krypton respectively. Several reactions are indicated.

The authors also bombarded thorium with fast neutrons from a lithium-deuterium source and found various radioactive components to be present in the alkali metal and alkaline earth metal precipitate.

1411: J. L. Snoek: Magnetic studies in the ternary system Fe-Ni-Al (Physica **6**, 321 - 331, Apr. 1939).

Measurements of the internal demagnetization show that alloys of different compositions upon slow cooling become heterogeneous and change from the composition two atoms of iron against one of Ni and one of Al to practically pure Ni-Al. After quenching at 1 200 °C and annealing at 500 °C the magnetic saturation is practically proportional to the iron content. When the alloys are cooled slowly to 500 °C and annealed at that temperature, a disturbance occurs between 10 and 60 atom per cent of iron which may be ascribed to a facecentred phase.